Electronic Supplementary Material (ESI) for Dalton Transactions.

Supporting Information

Ruthenium(II) *p*-Cymene Complexes of a Benzimidazole based Ligand Capable of VEGFR2 Inhibition: Hydrolysis, Reactivity and Cytotoxicity Studies

*Sudipta Bhattacharyya, Kallol Purkait, Arindam Mukherjee**

Department of Chemical Sciences, Indian Institute of Science Education and Research Kolkata, Mohanpur, Nadia-741246, India

Table of Contents

Compound interaction with CT DNA

Preparation of stock DNA solution

A concentrated stock solution of CT DNA was prepared in 50mM Tris–HCl/50 mM NaCl using MiliQ water (pH 7.4). DNA concentration was determined by measuring absorbance at 260 nm (CT DNA ε_{260} = 6600 M^{-1} cm^{-1}).[1] The CT DNA was found to be sufficiently free of protein since the absorbance ratio at 260 and 280nm was found to be ca. ~1.9.[2] The stock DNA solution was stored at 4°C and used within four days.

Binding studies with CT DNA

Stock solution of compounds were prepared in tris buffer–DMF (9:1 v/v). Interaction of compound **1 - 3** with CT DNA were measured with UV-vis spectroscopy using the above DNA solution. Spectroscopic titrations were carried out at room temperature. The concentration of **1 - 3** for the binding experiments were fixed to 3×10^{-5} M. The change in the absorbance was monitored with subsequent addition of an aliquot of CT DNA (4µL, [DNA] = 1×10^{-3} M) in both the sample and the reference cuvette. All the titration spectra were recorded after equilibration of the mixture for 5 min (post addition). Addition was continued until there was no visible change in the absorbance found for atleast three successive additions.

Gel electrophoresis

Electrophoretic mobility experiments were carried out by agarose gel electrophoresis using pBR322 plasmid DNA (Thermo Fisher Scientific). pBR322 DNA (30 µM with respect to base pair) was incubated with different molar ratio of compounds ([Compound]/[DNA]) r_b = 0.03 -1.66 in 50mM Tris-HCl buffer containing 4mM NaCl (pH 7.2). Test compounds were initially dissolved in 1: 9 DMF-Tris-HCl solution and diluted sufficiently so that final DMF concentration remained < 0.2 %. Incubation was continued up to 4h at 37 °C in dark then loading dye was added to it (2 µL, 0.05% bromophenol blue, 30mM EDTA, 40% glycerol,

0.05% xylene cyanol FF). Samples were subjected to electrophoresis in a 1% agarose gel in 1X TAE buffer (Tris-HCl, acetic acid and EDTA) for 3h at 60V. The gel was then stained with 0.5µg/mL ethidium bromide and visualised using Gel Documentation system (Bio-Rad).

In *vitro cytotoxicity* assay

Cell lines and culture conditions

The human carcinoma cell lines used are of adherent nature and epithelial in morphology. MCF-7 (human breast carcinoma), LNCaP (human metastatic prostate carcinoma), MIA PaCa-2 (human pancreatic carcinoma), HepG2 (Human hepato carcinoma) cell lines were procured from NCCS Pune, India (originally from ATCC). Cells were grown in T75 culture flasks as adherent monolayer in DMEM media supplemented with 10% heat-inactivated fetal bovine serum, 2 mM L-glutamine, 1mM Sodium Pyruvate (Only for HepG2) and 100 units of penicillin, 100 µg mL^{-1} of streptomycin. Cultures were cultured at 37 °C in a humidified 5% CO_2 atmosphere. All cell lines were maintained at their logerthemic phase of growth before each experiment and plated when it reaches 70% of confluency.

Cell viability assay(MTT)

MTT (3-(4, 5- dimethylthiazol-2-yl)-2, 5-diphenyltetrazolium bromide)] assay was performed for HL, **1 -3** to determine and screen cell viability against different cell lines. Briefly, 6×10^3 cells/well, were seeded in 96-well plates in appropriate growth media (200 µL) and maintained at 37°C humidified 5% CO_2 atmosphere. After 48 h, culture media renewed with a fresh media and kept inside CO_2 incubator before compound treatment. Compound stock solutions were prepared in growth media or PBS (for cis-platin only) containing DMSO. Compounds were first solubilised in cooled DMSO and then complete media/PBS was added to it with constant homogenisation. Further dilutions were done directly from main stock such that the concentration of DMSO in well should not exceed 0.2%. Additions of compound solution in

well were completed within 5min of stock solution preparation in DMSO. Triplicate cultures were established for each treatment. Compound treatment was continued for 48h. After 48h the media containing compound was carefully removed and fresh complete media was added in replacement. To each well 20 μL of a 1 mg mL^{-1} MTT in 1X PBS was added and incubated for 3h at 37°C in 5% carbon dioxide atmosphere. After 3h the media was removed completely (almost) and 100 μL of DMSO (molecular biology grade) was added to each of the well. The plate was then shaken on a 96-well plate shaker to homogenise the solution (dye). Absorbance of the purple solution of formazan in each well was measured at 515 nm [3, 4] in BIOTEK ELx800 plate reader. The live cell content which is proportional to the mean absorbance for each drug dose was expressed as cell survival obtained with respect to control experiment (in triplicate) and plotted against respective drug concentration. IC_{50} value represents the drug concentration that reduces the cell survival to 50% with respect to the controls. Cis-platin was used as positive control in this experiment. For experiment with addition of external GSH, an aqueous degassed solution of GSH was prepared in water and added to each well before addition of complex solution. Final concentration of GSH in each well was maintained at 1mM.

Determination of intracellular Reactive Oxygen Species (ROS)

Determination of ROS formed upon compound treatment was assayed by both FACS and microplate based assay. MCF-7 cells were cultured in 24 well plate (for microplate based assay)/90mm tissue culture petri dishes (for FACS analysis) and treated with compound **1 -3** for 10 h. As soon as compound treatment was over, media containing compounds were removed and cells were thoroughly washed with pre warmed (37°C) 1X PBS (pH=7.2) twice. After that cells were incubated with DCFH-DA solution (1 μM in 1X PBS, pH=7.2) for 15 min in dark. Excess DCFH-DA was washed out with consecutive washing with pre warmed 1X PBS (pH=7.2). For FACS analysis (FL-1 channel) a quick trypsinization was done before DCFH-DA treatment and analysed in 1X PBS within 30min. Whereas, for microplate based assay

direct fluorescence measurement was performed using FITC excitation. *tert*-butyl hydrogen peroxide was used as positive control in each experiment.

Cell cycle analysis by flowcytometry

1×10^6 MCF-7 cells per plate, were seeded in a 90 mm tissue culture petri dish in DMEM and cultured for 48h. Then requisite concentrations of **1-3** solution were added and incubated at previously described protocol after replacement of old culture media. After 24 h of exposure, cells were collected by gentle trypsinization and washed twice with cold 1X PBS (pH 7.2). Then 70% aqueous ice cold ethanol (Merck, ACS grade) was used to fix cells. Fixation was continued for overnight at 4ºC. Cell solution was then centrifuged and cell pellets were washed with 1X PBS to avoid excel ethanol. Cell pellets were resuspended in 500µL of 1X PBS solution containing propidium iodide (PI) (100 µg mL^{-1}) /RNaseA and incubated at 37ºC for ½ h in dark. Data was acquired in BD Biosciences FACSCalibur and percentage of cells in each phase was analysed by CellQuest Pro software.

Mitochondrial membrane potential change by flow cytometry

MCF-7 cells were grown on a 90 mm tissue culture petri dish at cell density of 5×10^5 for 48h in complete DMEM media. After removal of the media, a fresh media containing compound solution was added and incubated for additional 24h. Next the cells were harvested by trypsinisation and washed twice with pre warmed 1X PBS. Then cell pellet was resuspended (at a cell density of 1×10^6 cells/mL) in 500µL of JC-1 (10µg/mL) staining solution in PBS containing 10% FBS. The whole mixture was incubated for 15 min at 37°C in dark. The samples were then immediately analysed in BD Biosciences FACSCalibur . Population of cells having intact mitochondrial membrane potential was compared with the affected cell population by measurement of mean green and red fluorescence intensities.

DNA ladder assay for apoptosis detection

DNA ladder assay was performed with MCF-7. Briefly, 0.5×10^6 MCF-7 cells were seeded in 90 mm tissue culture petri-dish. Cells were allowed to grow for 48 h followed by media renewal. After that the cells were treated with **1** - **3** and incubated for additional 24 h. Next the cells were harvested by trypsinisation and centrifuged at 10000 rpm for 5 min. After this step all the treatments were done at 4ºC unless mentioned. Then, the cells were re-suspended in 0.5ml lysis buffer (20mM Tris-HCl (pH 7.4), 0.4mM EDTA, 0.25% Triton-X 100) followed by an incubation period of 15 min at room temperature. Lysed cells were centrifuged at 14000 rpm for 10 min. Supernatant was isolated and equi-volume of phenol-chloroform mixture was added to it. The bi-layer was vortxed for 1min and then centrifuged at 10000 rpm. The aqueous layer was isolated carefully without disturbing the interface. Aqueous supernatant was then treated with a mixture of 55µL of 5M NaCl and 550µL of ice cold isopropanol followed by incubation at –20ºC for overnight. Next day, the solution was centrifuged at 14000 rpm to obtain cell pellet and then the pellet was washed with 70% ice cold ethanol. The pellet was then air dried using compressed air stream. Dried pellet was re-suspended in 1X TE solution (10mM Tris-HCl (pH 8.0), 1mM EDTA) containing RNAse (150 µg/mL) and incubated at 37ºC for additional 15min. After that the whole solution mixture was centrifuged at 5000 rpm. The supernatant was loaded in 1.6% agarose gel containing EtBr (1.0 µg/mL) with bromophenol blue based loading dye and run at 60V for around 3h in 1X TBE (Tris-Borate-EDTA) buffer. Gel images were captured using a gel documentation system (Bio-Rad). The bands were identified with respect to the known base pair ladder (50bp step ladder, Sigma-Aldrich) run simultaneously in the gel.

Estimation of cellular Ru content

Quantification of total ruthenium uptake was performed with MCF-7 by ICP-MS analysis. Around 10^6 cells were seeded in a 90mm tissue culture petri dish and grown up to 48h in

DMEM media. Next the cells were treated with fresh media containing **1**-**3** (5μM) for additional 24h. Treated cells were washed and pelleted down by centrifugation at 10000 rpm for 10 min at 4ºC. Pelleted cells thus obtained were collected and air dried for 5 min. Dried pellets were treated with ultra pure grade 65% HNO_3 (Sigma) at 65ºC on a water bath for 6h. At end of incubation period, the whole solution was diluted to 10mL before analysis with MilliQ water containing 2% HNO_3 (Ultra pure grade). Samples were analysed on a Thermo Scientific XSERIES 2 ICP-MS instrument for ruthenium content with respect to Indium standard. All data obtained were subsequently subtracted from blank sample data (2% HNO_3 in MilliQ water). Sample data fitting was performed by standard curve drawn with different concentration range (10-200ppb) using standard ruthenium sample. Ruthenium content was expressed as nmol/10^6 cells. Triplicate experiments were performed to calculate standard deviations in data.

Caspase 3/7 activation assay

Activation of Caspase 3/7 due to complex treatment against MCF-7 was performed by Caspase 3 colorimetric detection kit (Sigma). As Caspase 3 and Caspase 7 are basically recognised by same substrate (DEVD) so common kit was used for Caspase 7 detection because MCF-7 does not have Caspase 3. The manufacturer's protocol was followed throughout the assay. MCF-7 as treated with **1**-**3** for 24h. Release of *p*-nitroaniline was monitored with time after caspase 3/7 substrate treatment with the cell lysate. The assay was performed following 96 well plate method and data recorded using ELISA plate reader at 405nm. Standard curve was drawn using known concentration of pNA to estimate amount of pNA release by Caspase 3/7.

Caspase 8 activation assay

Caspase 8 activation assay was performed by quantitative estimation of *p*-nitro aniline (pNA) release from pNA bound Caspase 8 substrate colorimetrically. This experiment has been

performed using Caspase 8 detection assay kit from Sigma Aldrich and kit protocol has been followed throughout. Complex treatment was same as for caspase 3/7 assay. Cell lysate obtained was treated with Caspase 8 substrate bound with pNA. This assay was done in a 96-well plate. Data was collected at different time period by measuring absorbance at 405nm. Standard curve was drawn using known concentration of PNA to estimate amount of PNA release by Caspase 8.

Wound healing (scratch) assay

Effect of complex (**1**-**3**) treatment upon migration of MCF-7 cells has been probed by wound healing (scratch) assay.[5-7] In short, MCF-7 cells were seeded in a 6 well plate and grown for a monolayer formation. An artificial wound was created by making scratch in the middle of each well using a sterile sharp tip. Then each well containing scratched monolayer was incubated with different concentration of **1**-**3** up to 48 h and bright field images were captured at different time interval. After that complex containing media was removed carefully from each well and fresh media devoid of any complex replaced. Monitoring was continued up to 48 h after removal of complexes. Bright field images of the wound area were captured at regular time intervals to observe the closure of the wound due to the migration of the cells. The results were quantified using the ImageJ software by measurement of wound area.

Western blotting

HepG2 cells of 5 X 10^5 density were seeded on a 6 well tissue culture plate and treated with two different concentration of the HL and **1** for 24h. Then cells were washed with cold 1X PBS (pH 7.4) twice and lysed using 1X RIPA buffer (supplemented with protease inhibitor cocktail, Amresco) in ice cold condition. Cells were then centrifuged at 10000 rpm for 10 min at 4 °C. Supernatant was collected and protein content was quantified by Bradford assay. 50 µg of protein was loaded in each well of 10-12 % SDS-

PAGE after denaturation in 1X laemmli buffer at 95 °C. Protein bands were transferred on a PVDF membrane by semi-dry gel electrophoresis in 1X Transfer buffer followed by blocking with 5% BSA in 1X TBST for 1h at room temperature. Then membrane was incubated in primary antibody solution in 1X TBS containing 5% BSA for overnight at 4 °C. The primary antibody used with dilution ratio were: rabbit polyclonal anti-VEGFR2 (Abcam, 1:3000), mouse monoclonal anti-Ras (BD-bioscience, 1:2000), mouse monoclonal anti-Akt (BD-bioscience, 1:1500), mouse monoclonal anti-beta actin (Abcam, 1:5000). After overnight incubation, membranes were washed with 1X TBST for 1h at room temperature. Then membranes were incubated with secondary antibody solution in 1X TBS containing 3% BSA (goat anti-mouse HRP polyclonal, BD Bioscience or goat anti-rabbit HRP polyclonal, Abcam) for 1h at room temperature. Protein bands were visualized with Luminata Forte Western HRP substrate (Millipore) and chemiluminescence image was captured using Syngene G-Box apparatus. Protein loading was verified by β-actin levels in blot. Densitometric analysis was performed by Gene Tools software.

In ovo anti-vascularisation assay

Specific antigen free chicken eggs were purchased from local government poultry farm. Egg shell was opened on day 5 of incubation. Egg shell window was closed by a sterile tape and returned to a humidified BOD incubator maintained at 37 °C. Compound stock solution prepared in 10% DMSO-Phosphate buffered saline (4mM NaCl) was diluted sufficiently to keep final DMSO concentration of < 0.5 %. After 2h of incubation shell window was opened and 30 µg of compound was added over the growing blood vessels in three different zones. Initial picture was captured at that time point and incubation continued for additional 48h. After that shell window was opened picture was taken on the same zone. Aseptic conditions were

maintained throughout the experiment to avoid contaminations. In all cases chicken embryo were found to be healthy and live.

Table S1. Comparative change in ^{1}H NMR shifts in HL and **1-3** upon coordination with different halides.

		Chemical shift in ^{1}H NMR signal(δ/ppm)			
		HL	**1**	**2**	**3**
-CH $_{aliphatic}$	H1	7.92	8.02(s)	7.91(s)	7.94-7.91(m, 1H)
-$CH_{Pz(Coordinated)}$	H15	5.93	6.14(s)	6.17(s)	6.17(s)
	H5a H5b H5c	2.09	2.66(s)	2.68(s)	2.67(s)
	H6a H6b H6c	2.19	1.95(s)	1.99(s)	1.98(s)
Benzene ring	H9	7.61-7.22	7.79(d, *J*=8.12Hz)	7.81(d, *J*=7.71Hz)	7.79(d, *J*=8.22Hz)
	H10 H11	7.22-7.17	7.48-7.41(m)	7.47(td, *J*=15.12, 7.10 Hz)	7.52-7.42(m)
	H12	7.61-7.22	7.91(d, *J*=8.11Hz)	7.94(d, *J*=7.95Hz)	7.94-7.91(m, 1H)
-$CH_{Pz\ (Non-coordinated)}$	H3	5.93	6.41(s)	6.48(s)	6.49(s)
	H17	2.19	2.52(s)	Masked by solvent peak	Masked by solvent peak
	H18	2.09	1.93(s)	1.95(s)	2.09(s)
p-cymene	H20	-	5.79(d, *J*=6.08Hz)	5.83(d, *J*=6.09Hz)	5.92(dd, *J*=4.90, 8.11Hz 1H)
	H21	-	5.87(d, *J*=6.08Hz)	5.92(d, *J*=6.21Hz)	5.92(dd, *J*=4.90, 8.11Hz 1H)
	H23	-	5.55(d, *J*=5.98Hz)	5.63(d, *J*=6.37Hz)	5.73(d, *J*=5.87Hz)
	H24	-	5.38(d, *J*=6.07Hz)	5.57(d, *J*=6.01Hz)	5.68(d, *J*=6.11Hz)
	H25	-	2.24-2.15(m)	2.17-2.12(m)	2.18-2.15(m)
	H26	-	1.04(d, *J*=6.85Hz)	1.04(d, *J*=6.85Hz)	1.05(d, *J*=6.91Hz)
	H27	-	0.97(d, *J*=6.85Hz)	0.88(d, *J*=6.85Hz)	0.81(d, *J*=6.84Hz)
	H28	-	2.13(s)	2.12(s)	2.12(s)
-NH_{imd}		12.23	14.26(bs)	13.98(bs)	13.94(bs)

Table S2. Comparative change in ^{13}C NMR shifts in HL and **1-3** upon coordination with different halides.

		Chemical shift in ^{13}C NMR signal(δ/ppm)			
		HL	**1**	**2**	**3**
-CH aliphatic	C1	68.51	64.07	64.35	64.31
-$CH_{Pz(Coordinated)}$	C2	140.58	140.50	140.66	140.63
	C15	106.70	109.21	109.20	109.02
	C4	148.03	147.29	147.59	147.80
	C5	10.92	16.58	17.71	19.65
	C6	13.48	10.65	10.54	10.53
Benzimidazole ring	C7	142.52	144.06	144.02	143.86
	C8	134.60	132.17	106.65	107.38
	C9	112.14	113.51	113.67	113.62
	C10	121.49	125.04	125.17	125.18
	C11	122.71	123.40	123.36	123.09
	C12	119.05	120.29	121.04	122.23
	C13	134.60	157.18	158.02	158.92
-$CH_{Pz\ (Non-coordinated)}$	C14	140.58	141.35	142.24	143.41
	C3	106.70	109.64	110.01	110.17
	C16	147.32	148.18	148.45	148.55
	C17	10.92	11.81	11.84	11.84
	C18	13.48	17.66	17.89	18.50
p-cymene	C19	-	104.60	105.63	106.66
	C20	-	83.27	83.22	83.23
	C21	-	83.44	82.82	83.12
	C22	-	101.68	101.32	100.84
	C23	-	82.26	82.56	83.09
	C24	-	81.90	82.56	82.00
	C25	-	30.10	30.15	30.21
	C26	-	22.17	22.09	22.70
	C27	-	22.48	22.51	21.85
	C28	-	13.04	13.42	13.16

Table S3. Selected crystallographic information parameters for HL**, 1** and **2.**

	HL	**1**	**2**
Empirical Formula	$C_{18}H_{20}N_6$	$[C_{28}H_{34}ClN_6Ru](Cl)$	$[C_{28}H_{34}BrN_6Ru](Br)$
*F*w (g mol^{-1})	320.40	626.58	715.50
T(K)	100.01(1)	100.01(1)	100.01(1)
Crystal system	Monoclinic	Monoclinic	monoclinic
Space group	C2/c	$P2_1/n$	$P2_1/n$
a (Å)	19.4406(7)	14.396(3)	14.2731(4)
b (Å)	10.4285(3)	11.675(3)	11.5926(3)
c (Å)	16.9620(7)	18.230(4)	18.4878(5)
α (°)	90.00	90.00	90.00
β (°)	109.057(4)	112.062(5)	111.225(3)
γ (°)	90.00	90.00	90.00
V (Å^3)	3250.4(2)	2839.63	2851.53(13)
Z	8	4	4
D_c (g cm^{-3})	1.309	1.510	1.667
μ (mm^{-1})	0.083	0.770	3.381
F(000)	1360.0	1364.0	1432.0
Index ranges	$-24 \le h \le 22$, $-13 \le k \le 11$, $-18 \le l \le 21$	$-18 \le h \le 19$, $-15 \le k \le 15$, $-22 \le l \le 24$	$-14 \le h \le 17$, $-14 \le k \le 14$, $-23 \le l \le 18$
Reflections collected	10650	49599	23086
Independent reflections	3318[R(int) = 0.0319]	6916[R(int) = 0.0551]	5820[R(int) = 0.0351]
Data/restraints/parameters	3318/0/221	6916/0/341	5820/0/341
Goodness-of-fit[a] on F^2	1.085	1.076	1.044
R_1[b],wR_2[c] [I>2σ(I)]	0.0441/0.1067	0.0382/0.0812	0.0257/ 0.0680
Largest diff. peak/hole / e Å^{-3}	0.27/-0.27	0.461/-0.746	0.65/-0.69

[a]Goodness-of-fit=$[\Sigma w(F_o^2 - F_c^2)^2] / (N_{refln} - N_{params})]^{1/2}$, based on all data.[b]$R_1 = \Sigma(|F_o|-|F_c|)/|F_o|$. [c]w$R_2 = [R[\Sigma (F_o^2 - F_c^2)^2] / R[\Sigma(F_o^2)^2]]^{1/2}$.

Table S4. Selected bond distances (Å) and angles (°) of HL**, 1** & **2.**

	HL	**1**	**2**
Ru(1)-N(1)	-	2.152(2)	2.137(2)
Ru(1)-N(3)	-	2.101(2)	2.088(2)
Ru(1)-X(1)	-	2.4063(9)	2.5393(3)
Ru(1)-C_{pcy} (shortest)	-	2.173(2)	2.180(3)
Ru(1)-C_{pcy} (longest)	-	2.230(3)	2.238(3)
N(1)-N(2)	1.370(2)	1.385(3)	1.385(3)
N(5)-N(6)	1.370(2)	1.369(4)	1.370(3)
N(2)-C(1)	1.443(2)	1.441(4)	1.438(3)
N(3)-C(7)	1.319(2)	1.318(3)	1.325(3)
N(4)-C(7)	1.355(2)	1.342(3)	1.340(3)
N(5)-C(1)	1.471(2)	1.482(3)	1.476(3)
N(1)-Ru(1)-N(3)	-	83.88(9)	84.29(8)
N(1)-Ru(1)-X(1)	-	84.79(6)	85.13(6)
N(3)-Ru(1)-X(1)	-	84.13(6)	84.17(6)
N(1)-N(2)-C(1)	120.27(13)	123.2(2)	123.6(2)
N(2)-C(1)-C(7)	114.54(13)	110.8(2)	110.7(2)
N(3)-C(7)-C(1)	120.16(14)	126.1(2)	126.2(2)
N(3)-C(7)-N(4)	114.25(14)	112.5(2)	112.7(2)
N(5)-C(1)-C(7)	110.50(13)	114.8(2)	114.6(2)
N(5)-C(1)-N(2)	111.20(13)	110.6(2)	110.6(2)

Table S5. Possible speciation of complexes inDMSO- Phosphate buffer (2:8 v/v) pD= 7.4 containing 4mM NaCl at 25° C observed in ESI-MS.

	5min	24h	
Species	Observed	Observed	Simulated
[**1** –H – *p*-cym + K]$^+$	495.08	495.09	495.00
[**1** –H –Cl]$^+$	555.18	555.18	555.18
[**1**]$^+$	591.16	591.16	591.16
[**1** –H + Na]$^+$	613.14	613.14	613.14
[**1** –H + K]$^+$	629.11	629.12	629.11
[**1** –H – Cl + DMSO + H_2O] $^+$	-	651.25	651.21
Dimer [$C_{56}H_{66}ClN_{12}Ru_2$]$^+$	1145.33	1145.34	1145.33
[**2** –H –*p*-cym +H_2O + Na]$^+$	541.04	541.04	540.99
[**2** –H –Br]$^+$	555.18	555.18	555.18
[**2**]$^+$	635.11	635.12	635.10
[**2** –H + Na]$^+$	657.09	657.09	657.09
Dimer [$C_{56}H_{66}ClN_{12}Ru_2$]$^+$	1145.33	1145.33	1145.33
[**3** –H –I]$^+$	555.18	555.18	555.18
[**3** –H – p-cym+ K]$^+$	587.02	587.02	586.93
[**3**]$^+$	683.09	683.09	683.09
[**3** –H + Na]$^+$	705.07	705.07	705.07
[**3** –H + K]$^+$	721.04	721.05	721.04
Dimer [$C_{56}H_{66}ClN_{12}Ru_2$]$^+$	1145.34	1145.33	1145.33

Table S6. ESI-MS speciation data of complexes in DMSO-Phosphate buffer (2:8 v/v) pD= 7.4 containing 4mM NaCl in presence of 10 eq. of GSH at 25° C.

Complex 1			
	5min	24h	
Species	Observed	calculated	Calculated
$[L – Pz –H –D]^+$	-	226.12	226.12
$[GSH + H]^+$	308.03	-	308.09
[HL + H]+	321.18	321.18	321.18
$[HL – H + D + H]^+$	-	322.19	322.19
$[GSH +Na]^+$	330.07	330.07	330.07
$[HL + Na]^+$	-	343.16	343.16
$[GSH + Na]^+$	346.03	-	346.05
$[\mathbf{1} –H – p\text{-cym} + K]^+$	495.00	-	495.00
$[\mathbf{1} – p\text{-cym} –H +D + H_2O]^+$		496.09	496.06
$[\mathbf{1} –H –Cl]^+$	555.17	-	555.18
$[\mathbf{1}]^+$	591.15	-	591.15
$[\mathbf{1} –HL + GS(O)]^+$	-	592.17	592.16
$[GSSG + H]^+$	-	613.17	613.16
$[2GSH +H]^+$	615.17	-	615.17
$[2GSH +Na]^+$	635.14	-	637.15
$[\mathbf{1} –Cl + GS]^+$	862.26	-	862.26
$[\mathbf{1} + GSH]^+$	898.23	-	898.23
Complex 3			
$[L – Pz –H –D]^+$	-	226.12	226.12
$[GSH + H]^+$	308.03	-	308.09
[HL + H]+	321.18	-	321.18
$[HL – H + D + H]^+$	-	322.19	322.19
$[GSH +Na]^+$	330.07	330.07	330.07
$[HL + Na]^+$	343.16	343.16	343.16
$[\mathbf{3} –H –I]^+$	555.18	-	555.18
$[\mathbf{3} –HL – I +Cl + GS(O)]^+$	-	592.17	592.16
$[\mathbf{3}]^+$	683.09	-	683.09
$[GSSG + H]^+$	-	613.16	613.16
$[\mathbf{3} –I + GS]^+$	862.27	-	862.26
$[\mathbf{3} –H – p\text{-cym} + K]^+$	587.03		586.93
$[\mathbf{3} –H +D]^+$	-	684.10	684.09

Table S7. CT DNA interaction parameters of **1-3**.

	K_b x10^3(M^{-1})	ΔT_m (ºC)
1	3.19(4)	3
2	1.07(2)	1
3	2.54(1)	2

Table S8. Comparison of selected bond distances (Å) and angles (°) of HL and its metal complexes determined experimentally (except **3**) and theoretically.[a]

	HL		**1**		**2**		**3**
	SCXRD	DFT	SCXRD	DFT	SCXRD	DFT	DFT
Ru(1)-N(1)	-	-	2.152(2)	2.15982	2.137(2)	2.15867	2.16998
Ru(1)-N(3)	-	-	2.101(2)	2.10326	2.088(2)	2.10493	2.11681
Ru(1)-X(1)	-	-	2.406(9)	2.45093	2.539(3)	2.58182	2.78517
Ru(1)-C_{pcy}	-	-	2.173(2)	2.2301	2.180(3)	2.23167	2.23041
Ru(1)-C_{pcy}	-	-	2.230(3)	2.3094	2.238(3)	2.31225	2.35919
N(1)-N(2)	1.3708(18)	1.36805	1.385(3)	1.37682	1.385(3)	1.37787	1.38238
N(5)-N(6)	1.3704(18)	1.36280	1.369(4)	1.36462	1.370(3)	1.36480	1.36192
N(2)-C(1)	1.443(2)	1.45186	1.441(4)	1.44013	1.438(3)	1.43999	1.44384
N(3)-C(7)	1.319(2)	1.31761	1.318(3)	1.32333	1.325(3)	1.32334	1.32593
N(4)-C(7)	1.355(2)	1.36592	1.342(3)	1.35893	1.340(3)	1.35874	1.35967
N(5)-C(1)	1.471(2)	1.46688	1.482(3)	1.47779	1.476(3)	1.47927	1.47249
N(1)-Ru(1)-N(3)	-	-	83.88(9)	84.37189	84.29(8)	84.76070	84.88917
N(1)-Ru(1)-X(1)	-	-	84.79(6)	84.77317	85.13(6)	85.04050	71.25817
N(3)-Ru(1)-X(1)	-	-	84.13(6)	84.63486	84.17(6)	84.71119	69.04869
N(1)-N(2)-C(1)	120.27(13)	120.91753	123.2(2)	123.50118	123.6(2)	123.64976	124.06152
N(2)-C(1)-C(7)	114.54(13)	113.80895	110.8(2)	111.10214	110.7(2)	111.28461	112.31620
N(3)-C(7)-C(1)	120.16(14)	121.72712	126.1(2)	126.77617	126.2(2)	126.91075	127.34576
N(3)-C(7)-N(4)	114.25(14)	113.79355	112.5(2)	111.47030	112.7(2)	111.49662	111.83014
N(5)-C(1)-C(7)	110.50(13)	111.16788	114.8(2)	115.03339	114.6(2)	114.94542	114.48814
N(5)-C(1)-N(2)	111.20(13)	111.99096	110.6(2)	111.29396	110.6(2)	111.35603	111.90722

[a] experimentally from crystal structure and theoretically from DFT calculation (details in experimental section).

Table S9. Selected GOLD docking parameters and corresponding interacting residues in VEGFR2 using the energy minimised structure of native bound inhibitor extraction. Hydrogen bonding distances are shown in parenthesis (Å unit) (PDB ID: 1YWN).

Molecule Name	GOLD Score	External vdw	H-bonding Residue[a]	Residues favouring hydrophobic interactions	RMSD (Å)
1	34.27	28.15	Leu838 (3.800) [C=O…H-C63, ∠117.40°] Lys866(3.800) [N-H…N3, ∠158.22°]	Val846, Lys866, Cys1043, Asn1031, Asp1044	5.2
2	40.54	29.84	Val846 (3.247) [C-H…Br, ∠154.86°] Glu883 (3.708) [CO_2^-…H-C31, ∠134.56°] Asn1031 (3.214) [=O…H-C62, ∠160.33°] Cys1043 (4.073) [S…H-C47, ∠160.33°]	Leu838, Lys866, Arg1030, Cys1043	6.4
3	38.78	32.96	Lys838 (3.659) [CH...I, ∠160.93°] Gly844 (3.074) [=O…H-C29, ∠137.92°] Val846 (3.260) [C-H…I, ∠116.31°] Glu883 (3.501) [CO_2^-…H-C66, ∠123.33°]	Gly841, Arg1030, Asn1031, Cys1043, Asp1044	5.2
[Ru(η^6-*p*-cym)(L)(OH_2)]$^{2+}$	32.35	24.04	Leu838 (3.074) [=O…H-C19, ∠127.14°] Asp1044 (4.005) [=O…H-C58, ∠136.14°]	Val846, Gly841, Asn1031, Cys1043	6.1
Ligand (L)	50.87	35.98	Glu883 (2.92) [CO_2^-…H-N1, ∠157.58°] Asp1044 (3.01) [N-H…N5, ∠153.41°]	Leu887, Val897, Cys1043, Asp1044	4.7
SU5416[b]	41.25	30.01	Glu883 (3.509) [C-H…O11, ∠130.22°] Asp1044 (3.972) [CO_2^-…H-C17, ∠125.01°] Asp1044 (2.600) [=O...H-C17, ∠115.39°]	ILE890, Glu883, Val897, Asp1044	3.34
Axitinib[c]	58.67	43.20	Phe843 (3.162) [=O…H-C23, ∠156.53°] Lys866 (2.819) [N-H…N24, ∠163.46°] Glu883 (3.530) [C-H...N25, ∠161.21°] Glu883 (2.624) [CO_2^-…H-N26, ∠137.95°] Glu883 (2.624) [CO_2^-…N25(lp) Asp1044 (2.822) [=O...H-C14, ∠131.96°] Asp1044(3.917) [=O…H-C18, ∠151.20°] Asp1044(2.949) [CO_2^-…H-N2, ∠162.47°]	Phe843, Ile866, Glu883, Cys1043, His1024	0.3

[a] bond distances shown in Å and angles shown in °, [b] (3-[(2,4-indolin-2-one), [c] N-methyl-2-[[3-[(E)-2-pyridin-2-ylethenyl]-1H-indazol-6-yl]sulfanyl]benzamide

Table S10. Selected GOLD docking parameters and corresponding interacting residues in VEGFR2 (native inhibitor bound structure) (PDB ID: 1YWN). Hydrogen bonding distances are shown in parenthesis (Å unit).

			Interacting Residues		
Molecule Name	GOLD Score	External vdw	H-bonding Residue[a]	Residues favouring hydrophobic interactions	RMS D (Å)
1	44.37	32.73	Gly839 (3.616) [C=O…H-C20, ∠151.46] Glu883 (3.39) [=O…H-C32, ∠122.41] Asn1031 (3.26) [=O…H-C63, ∠153.56]	Leu838, Val846, Asp1044	6.7
2	43.49	31.78	Val846 (2.398) [Br…H-CH_3, ∠154.94] Glu883 (3.512) [CO_2^-…H-C13, ∠134.40] Arg1030 (3.598) [=O…H-C62, ∠143.11]	Leu838, Phe843, Lys866, Cys1043	6.8
3	44.85	33.06	Arg840 (3.472) [=O…H-C58, ∠141.31] Phe843 (4.181) [=O…H-N5, ∠132.10]	Gly844, Arg1030, Asn1031, Asp1044	5.9
[Ru(η^6-*p*-cym)(L)(OH_2)]$^{2+}$	41.57	32.05	Glu883 (3.312) [CO_2^-…H-C56, ∠127.58]	Gly839, Lys866, Arg1030, Cys1043, Asp1044	6.4
Ligand (L)	50.40	38.33	Glu883 (2.92) [CO_2^-…H-N1, ∠157.58] Asp1044 (3.01) [N-H…N5, ∠153.41]	Lys866, Glu883, Leu887, Val897, Asp1044	2.6
SU5416[b]	37.59	27.36	Glu883 (4.097) [CO_2^-…H-C17, ∠145.94]	Glu883, ILE886, ILE890, Val897, Asp1044	6.2
Axitinib[c]	56.03	42.95	Leu838 (2.89) [C-H...O4, ∠136.92] Glu883 (2.624) [CO_2^-…H-N26, ∠137.95] Glu883 (2.624) [CO_2^-…N25(lp) Leu887(3.02) [=O…H-C8, ∠160.63]	Val846, Glu883, Cys917, His1024, Cys1043	0.3

[a] bond distances shown in Å and angles shown in °, [b] (3-[(2,4-indolin-2-one), [c] N-methyl-2-[[3-[(E)-2-pyridin-2-ylethenyl]-1H-indazol-6-yl]sulfanyl]benzamide

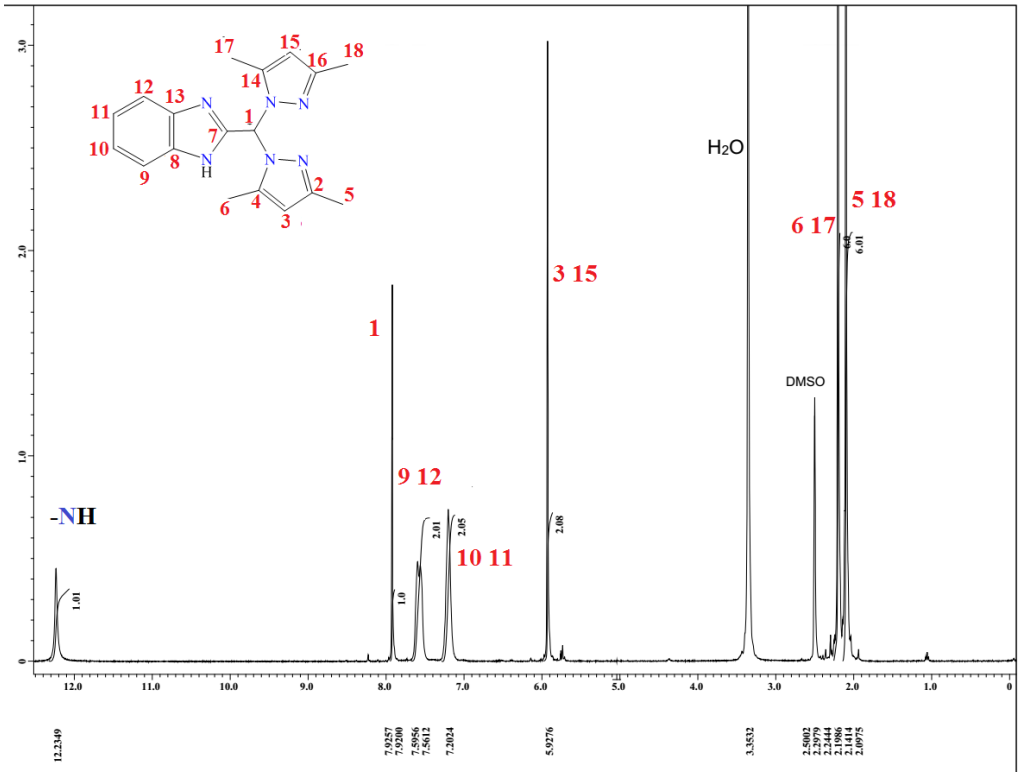

Figure S1. ^{1}H NMR spectra of HL in DMSO-d$_6$.

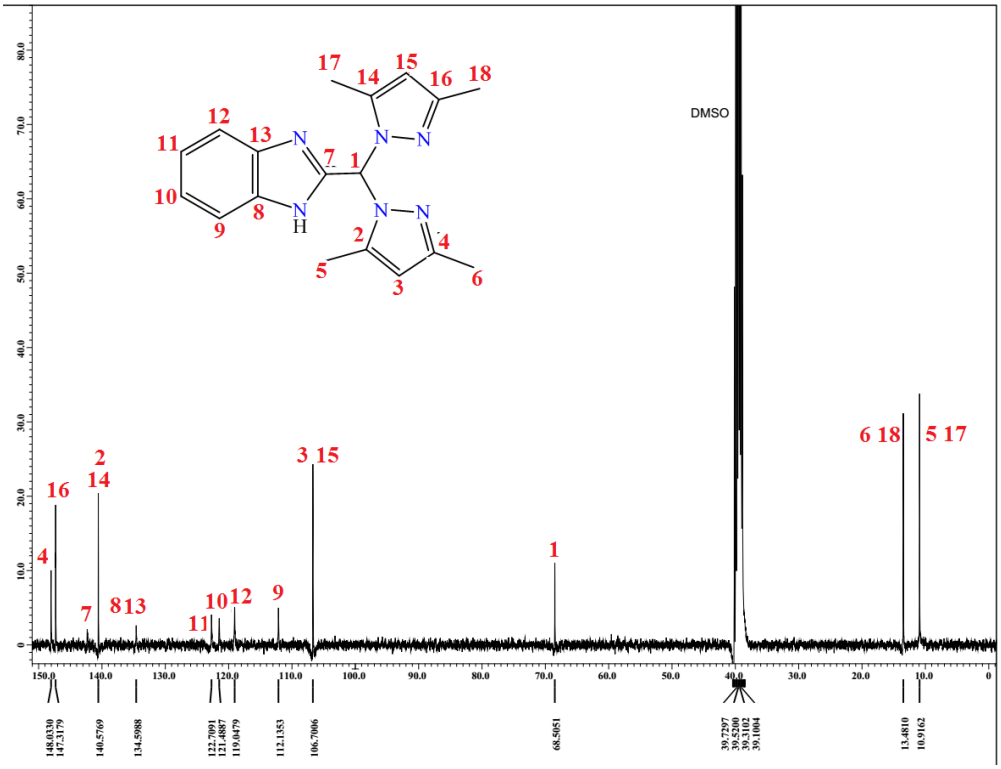

Fig. S2. ^{13}C NMR of HL in DMSO-*d*$_6$.

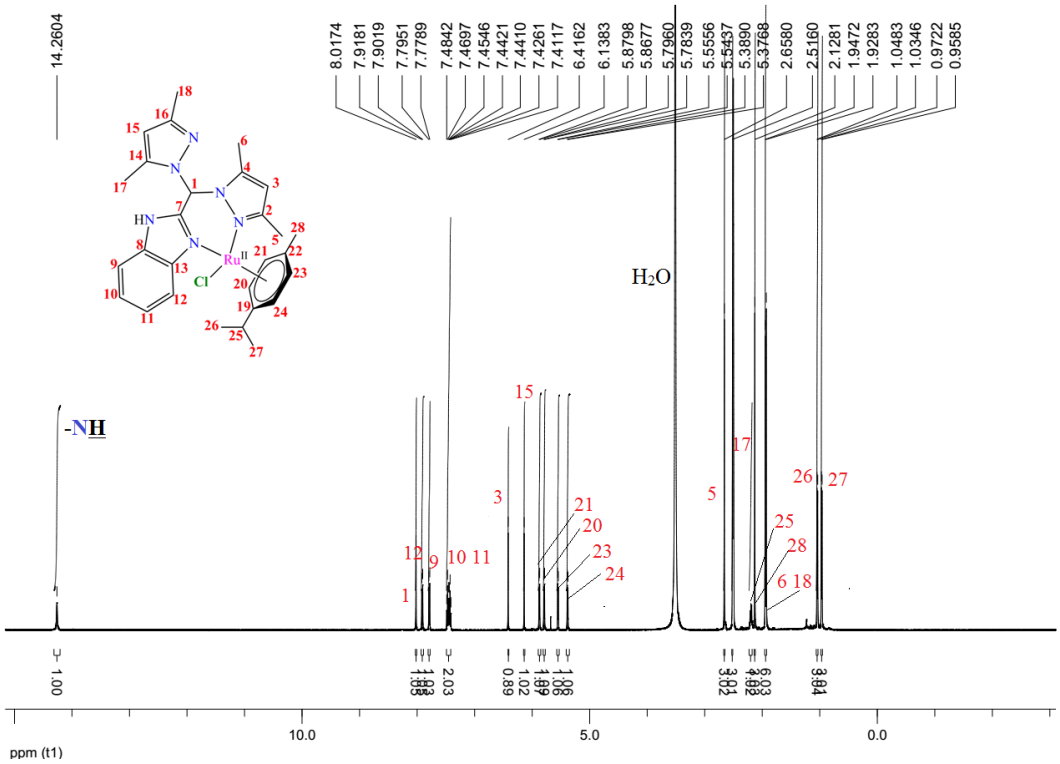

Fig. S3. ^{1}H NMR spectra of **1** in DMSO-d$_6$.

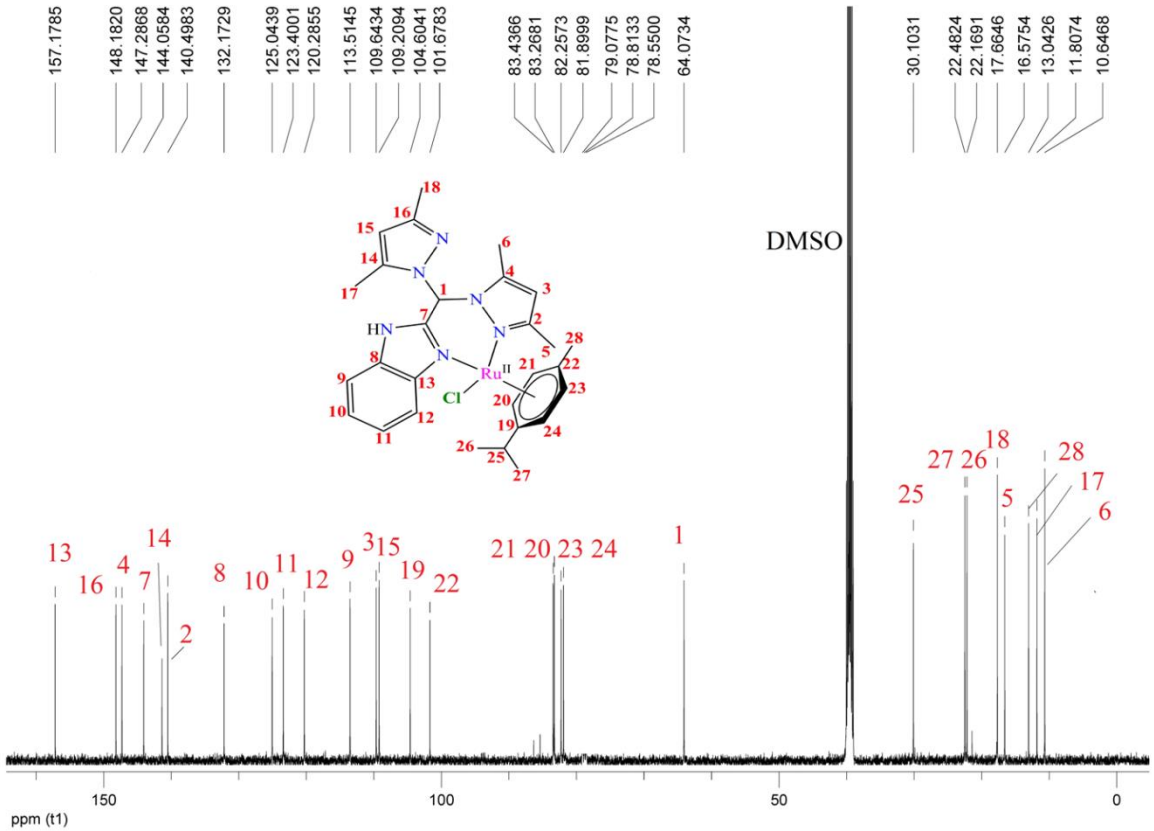

Fig. S4. ^{13}C NMR of **1** in DMSO-*d*$_6$.

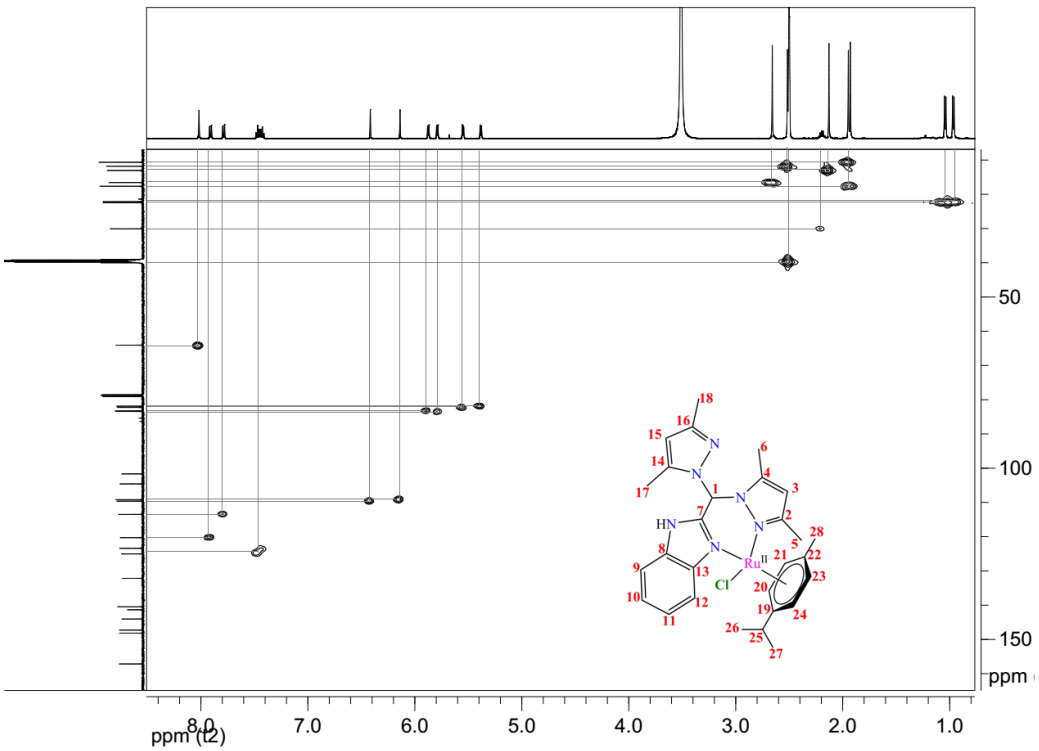

Fig. S5. HMQC of **1** in DMSO-d_6.

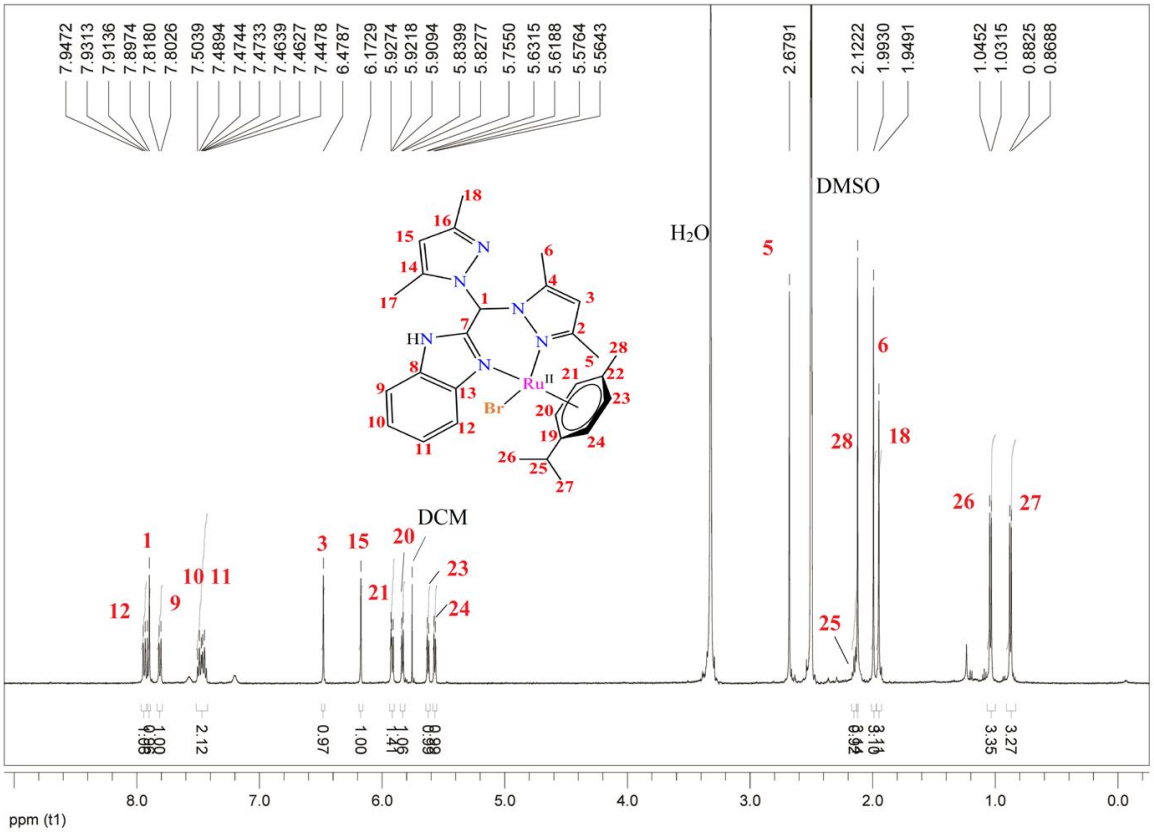

Fig. S6. ^{1}H NMR spectra of **2** in DMSO-d_6.

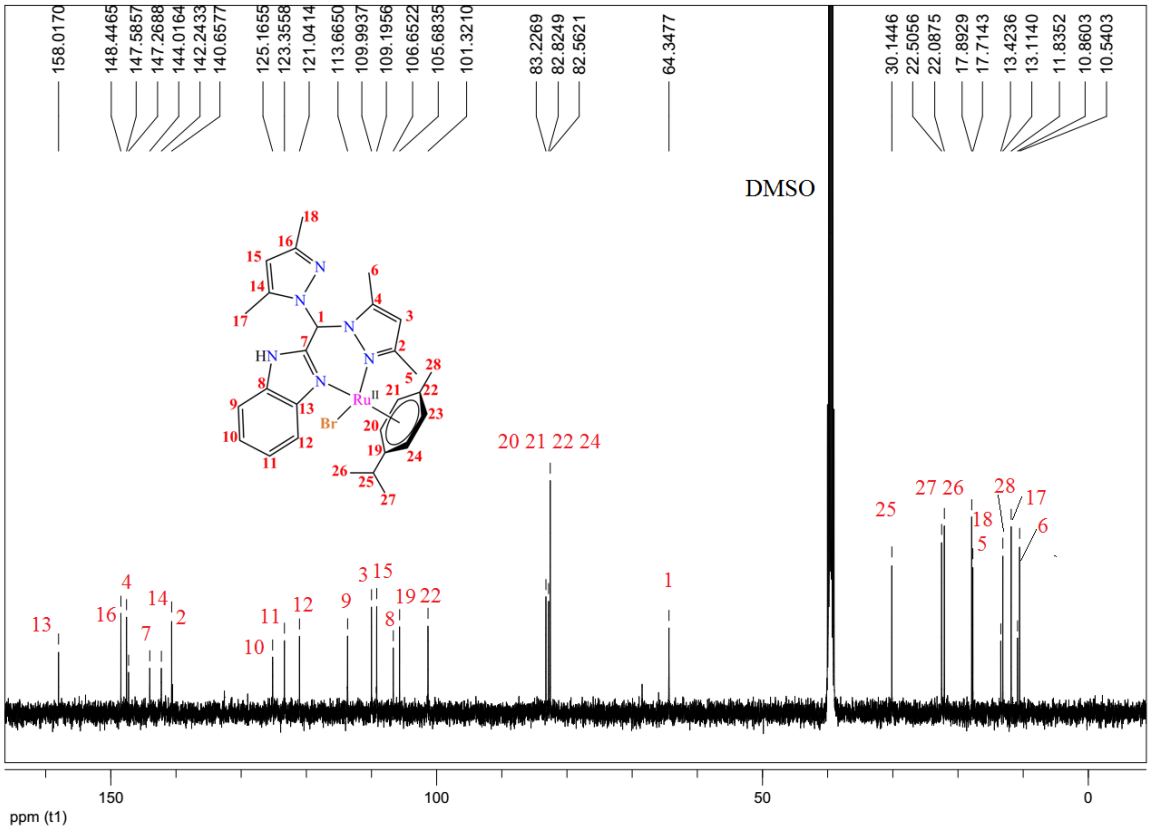

Fig. S7. ^{13}C NMR of **2** in DMSO-d_6.

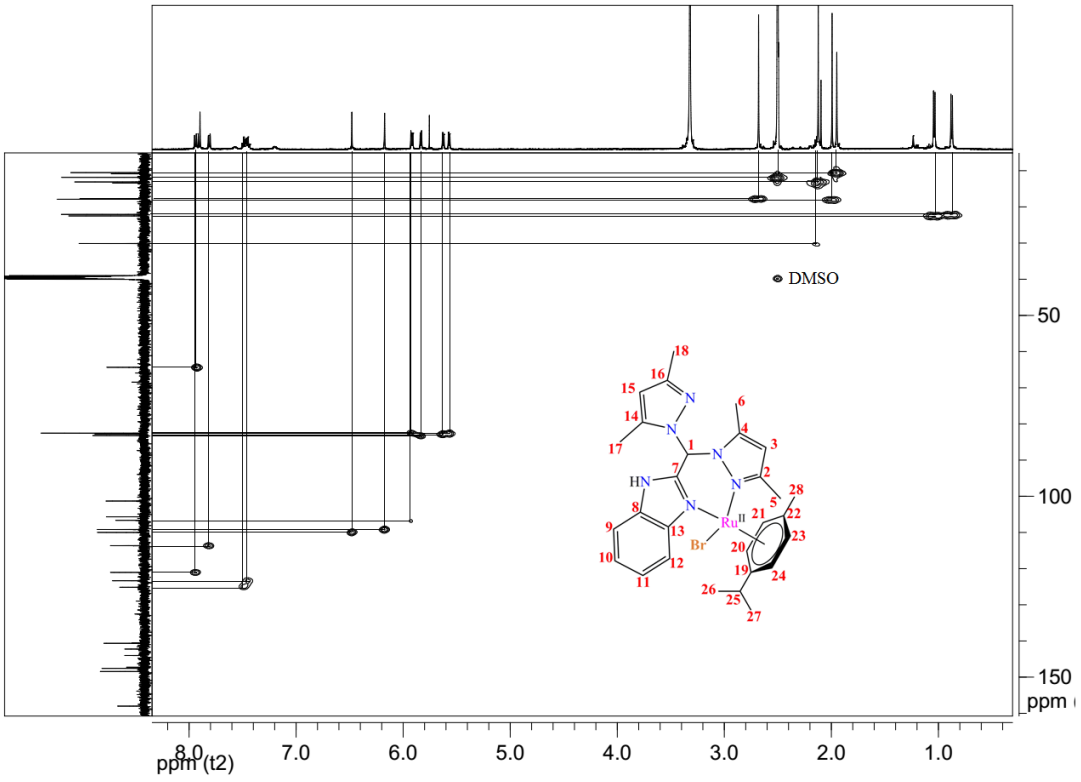

Fig. S8. HMQC of **2** in DMSO-d_6.

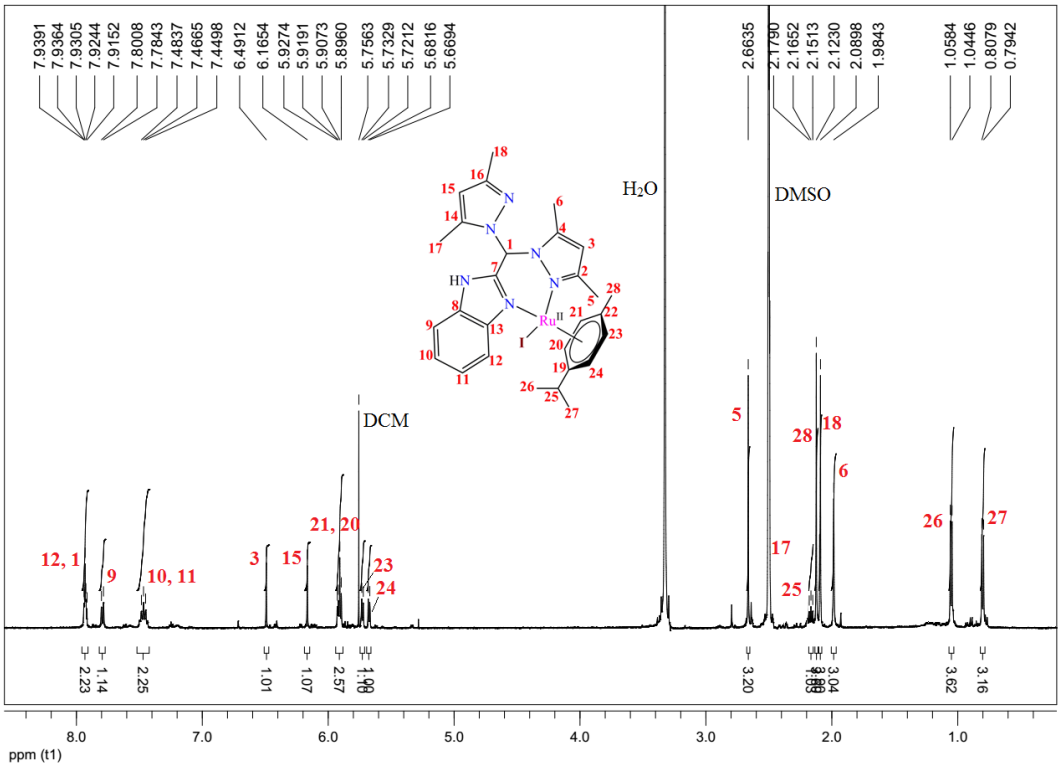

Fig. S9. ^{1}H NMR spectra of **3** in DMSO-d$_6$.

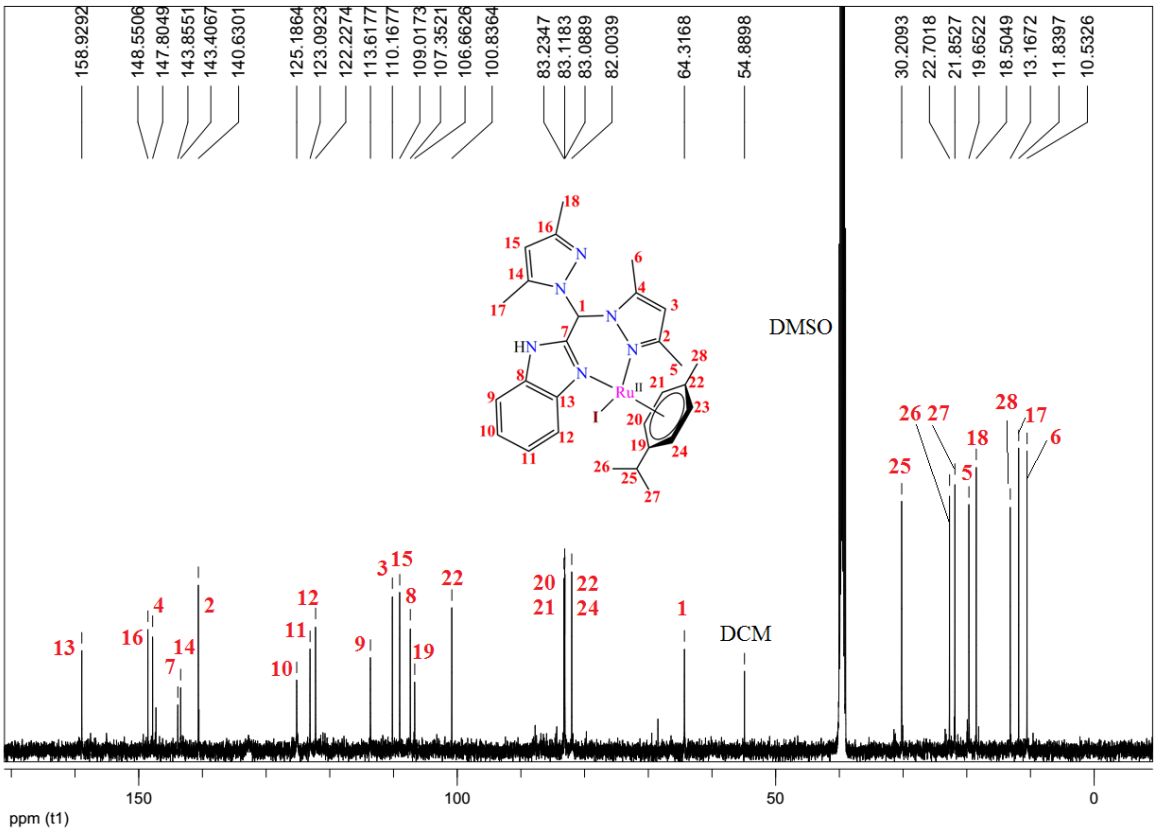

Fig. S10. ^{13}C NMR of **3** in DMSO-*d*$_6$.

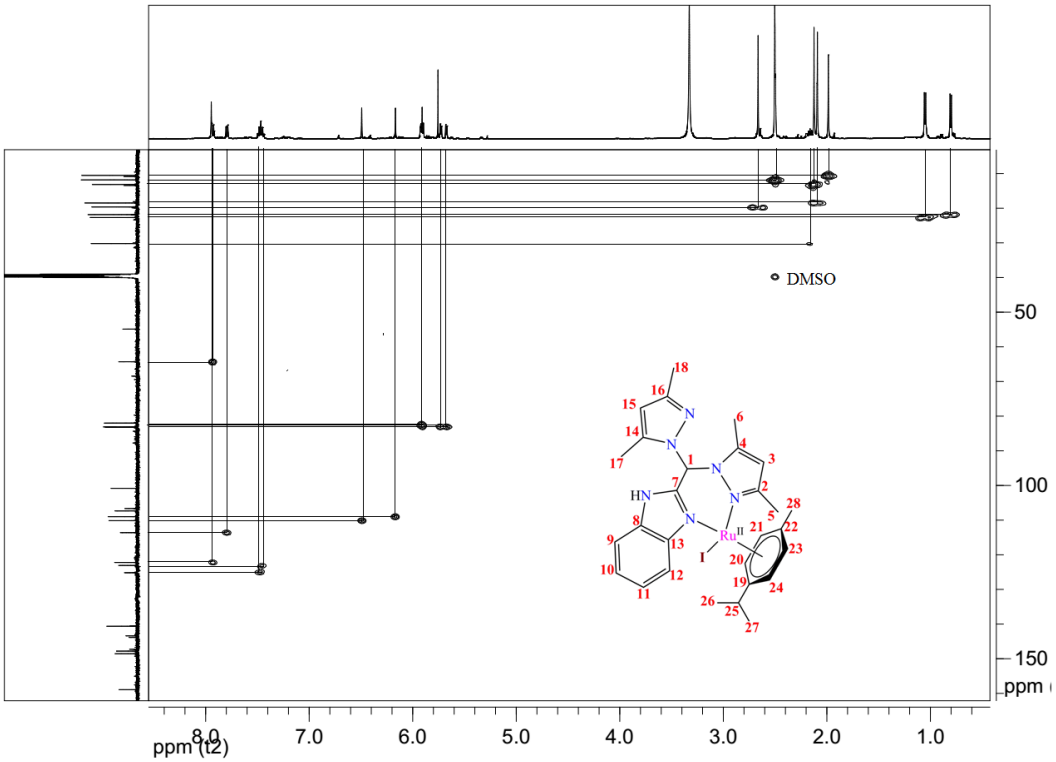

Fig. S11. HMQC of **3** in DMSO-d_6.

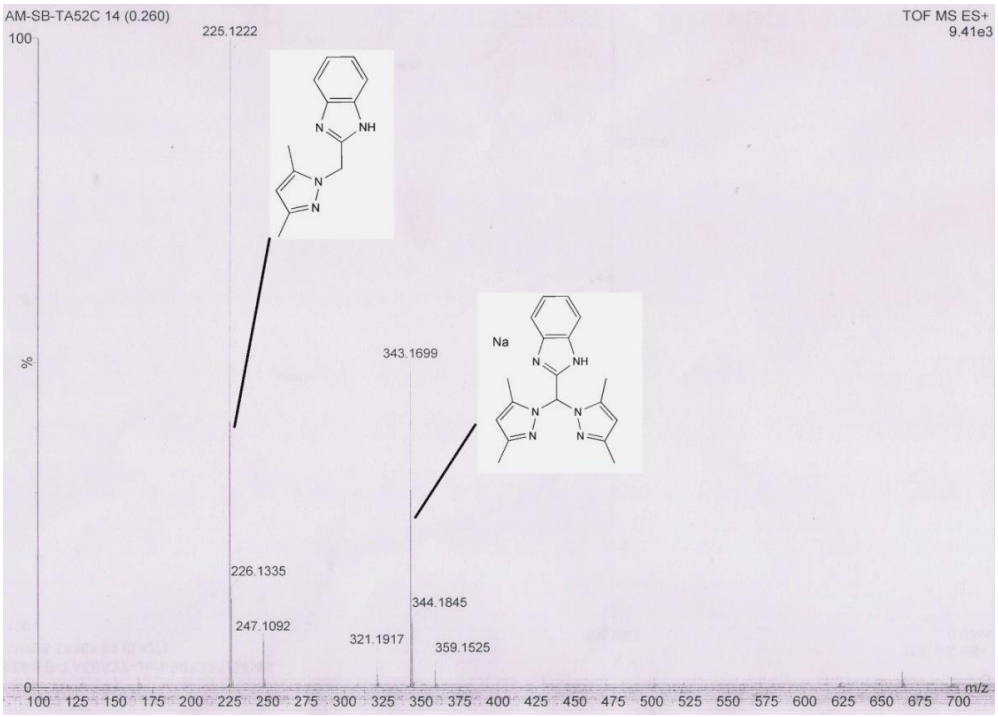

Fig. S12. ESI-MS (+ve mode) of HL in methanol.

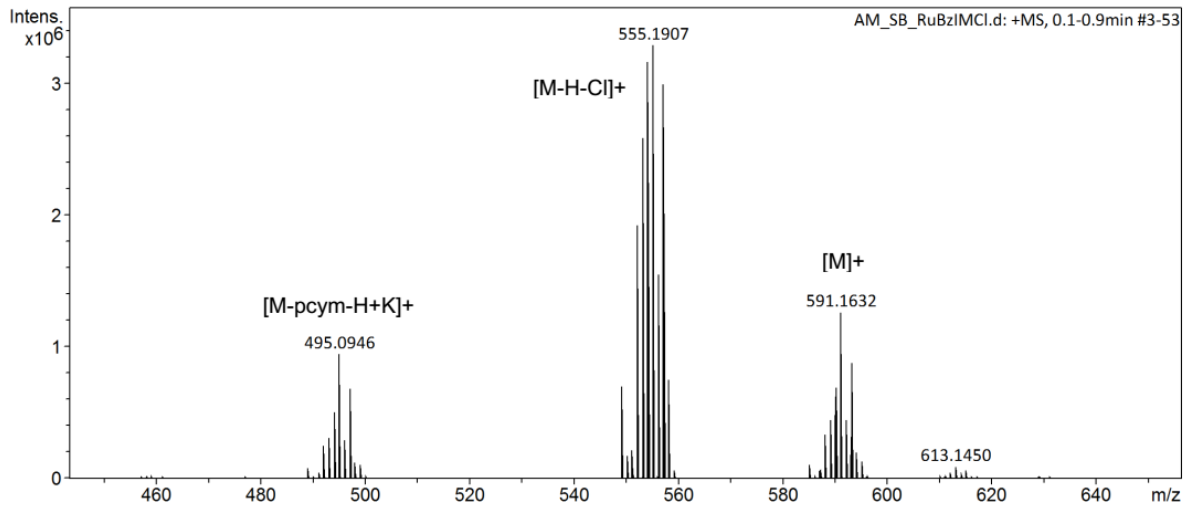

Fig. S13. ESI-MS (+ve mode) of **1** in methanol.

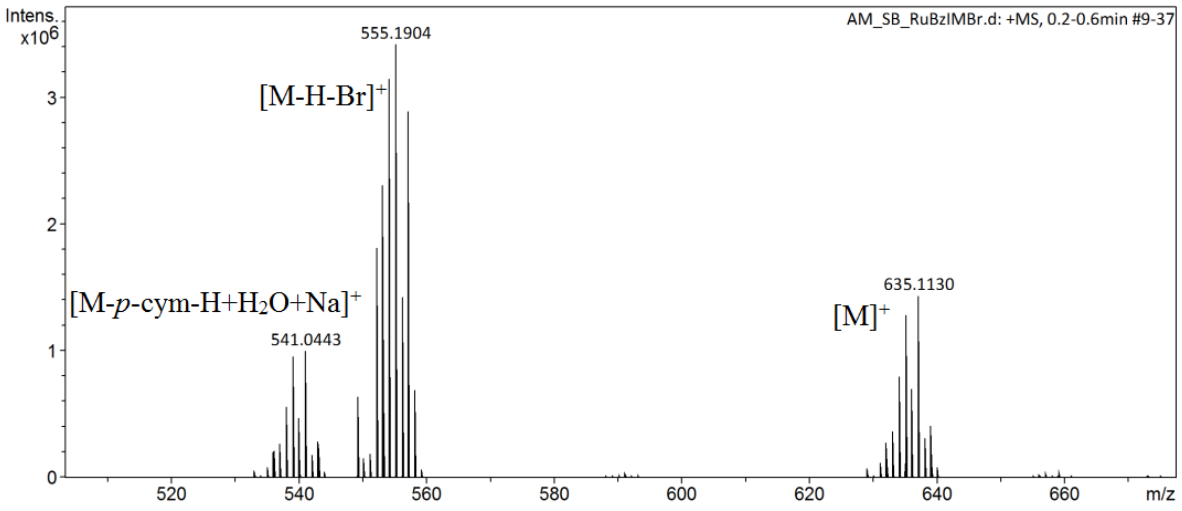

Fig. S14. ESI-MS (+ve mode) of **2** in methanol.

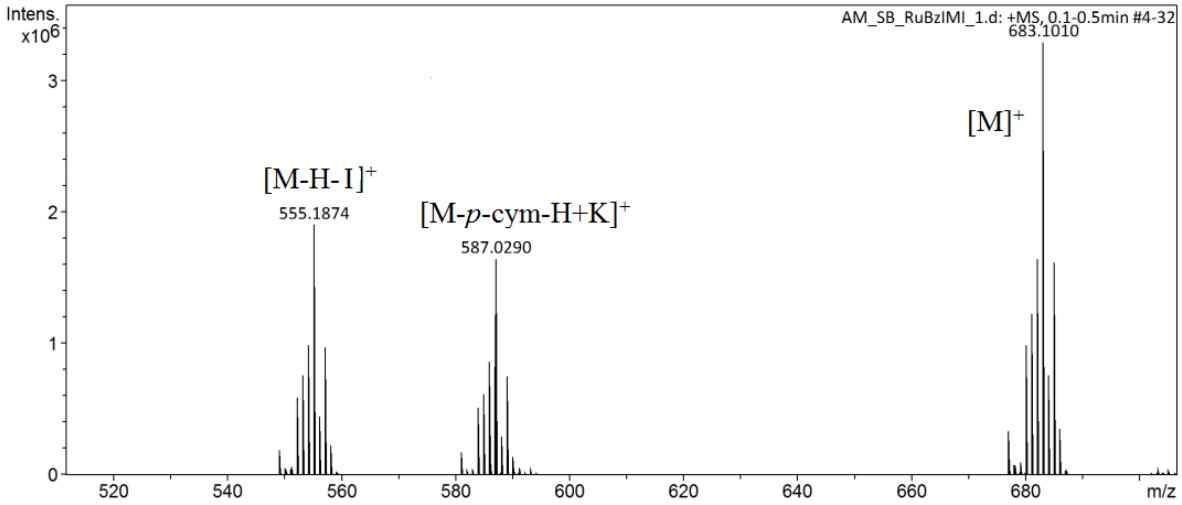

Fig. S15. ESI-MS (+ve mode) of **3** in methanol.

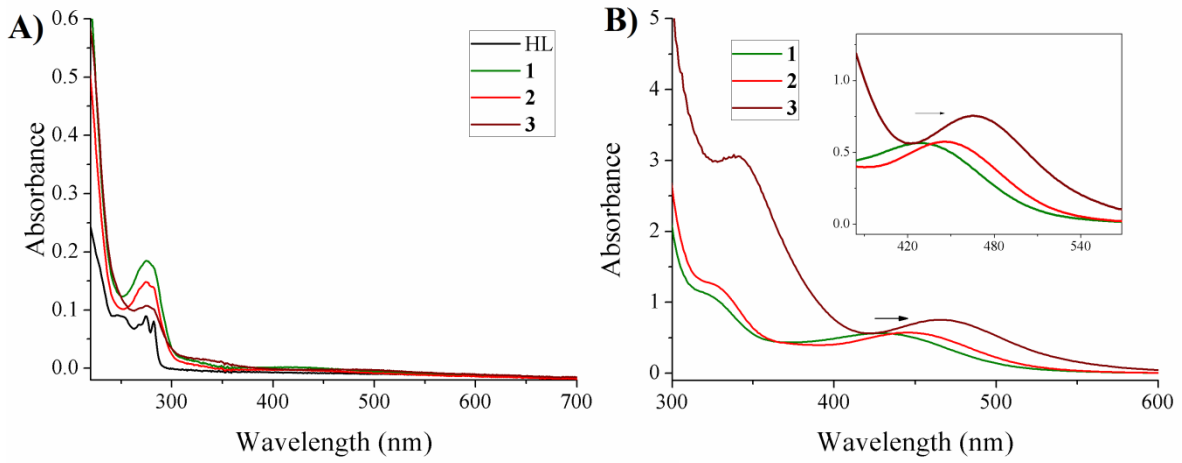

Fig. S16. Electronic spectral traces of A) HL, **1-3** (1 x 10^{-3}M) and B) ruthenium cantered band of **1-3** in methanol.

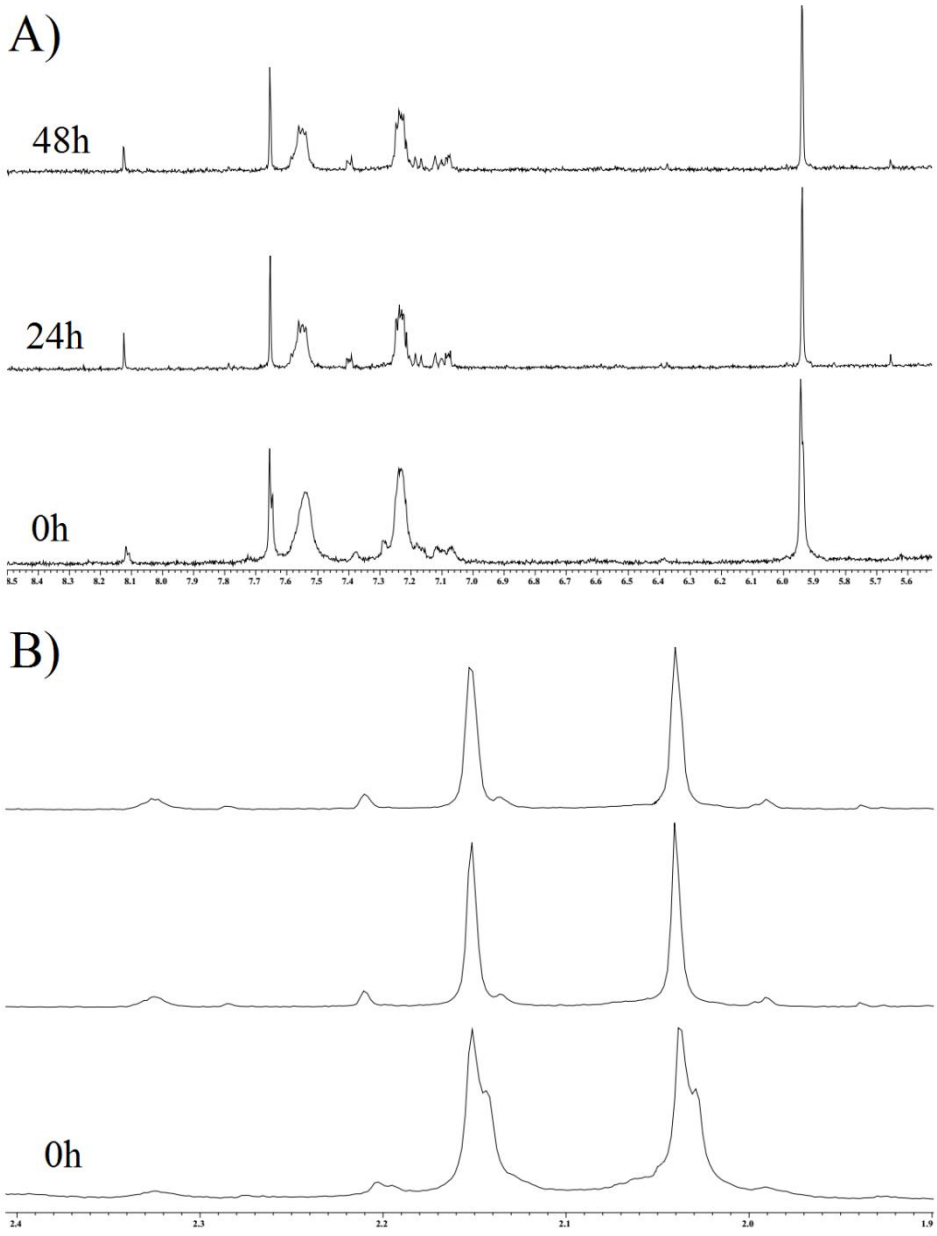

Fig. S17. Stability kinetics of HL in 2:8(v/v) DMSO-d_6 and 10mM phosphate buffer containing 4mM NaCl (pD = 7.4) by ^{1}H NMR at 25°C. A) Aromatic region and B) aliphatic region expansion.

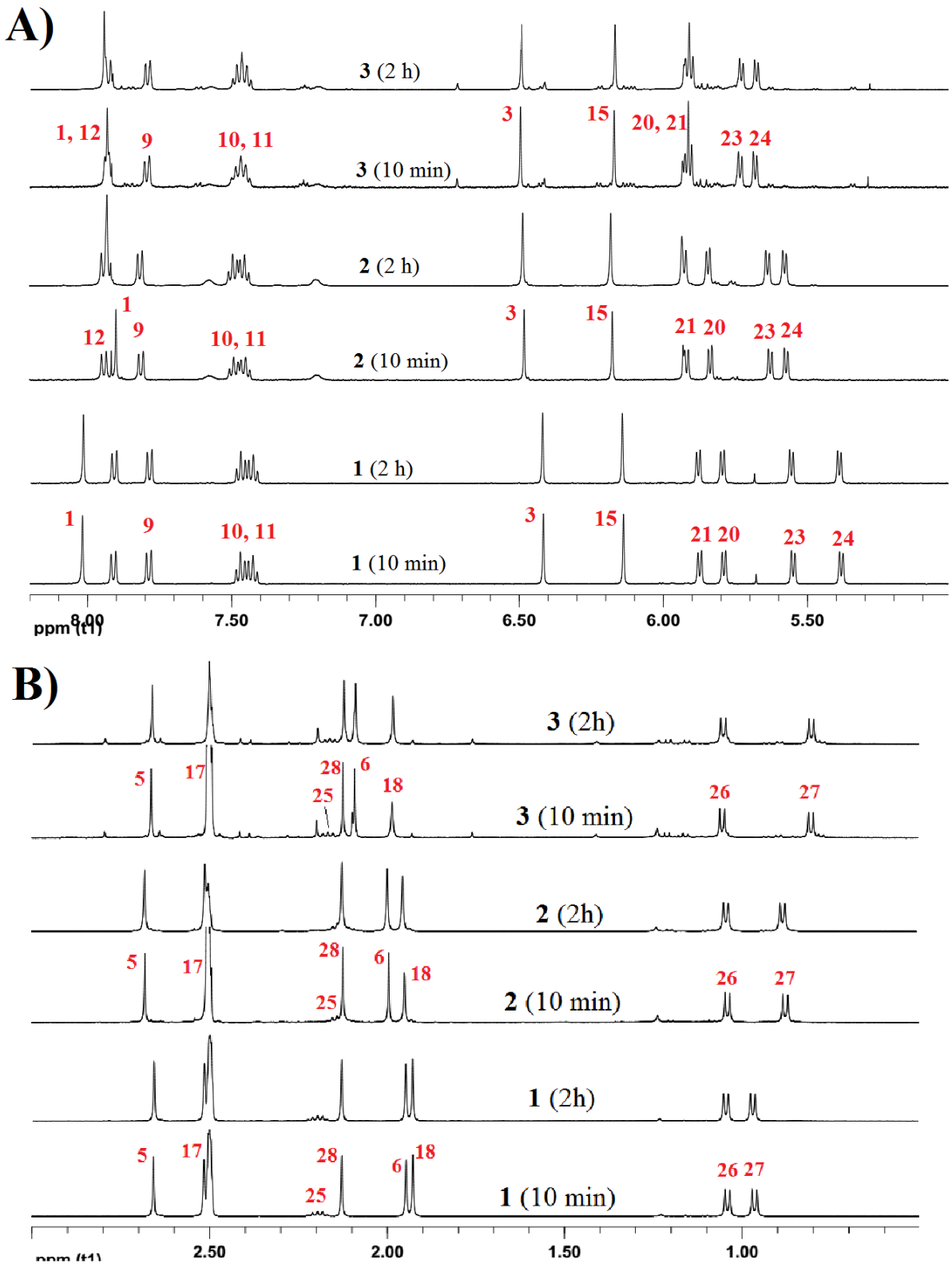

Fig. S18. Representative ^{1}H NMR stack of **1-3** in DMSO-d_6 recorded after 2 h of solution preparation. A) aromatic expansion and B) aliphatic expansion of spectra. Unaltered spectral position is indicative of stable nature of the metal complexes in DMSO.

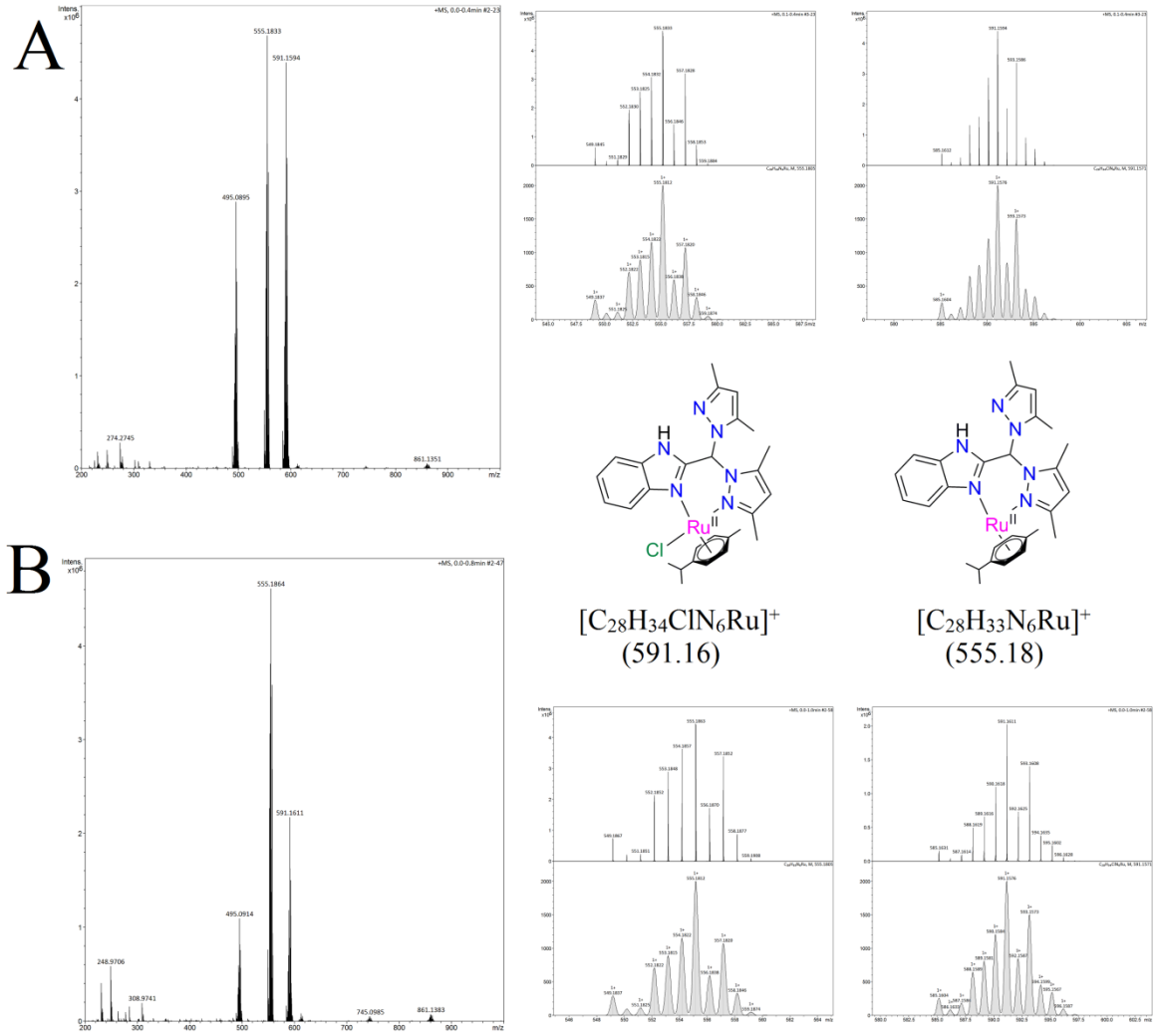

Fig. S19. ESI-MS (+ve mode) spectral traces of **1** in DMSO-d_6 and 10mM phosphate buffer containing 4mM NaCl (pD = 7.4) (2:8 v/v) mixture; A) after 5min and B) 24h of dissolution. Simulated spectra for species of interest are shown in right hand side.

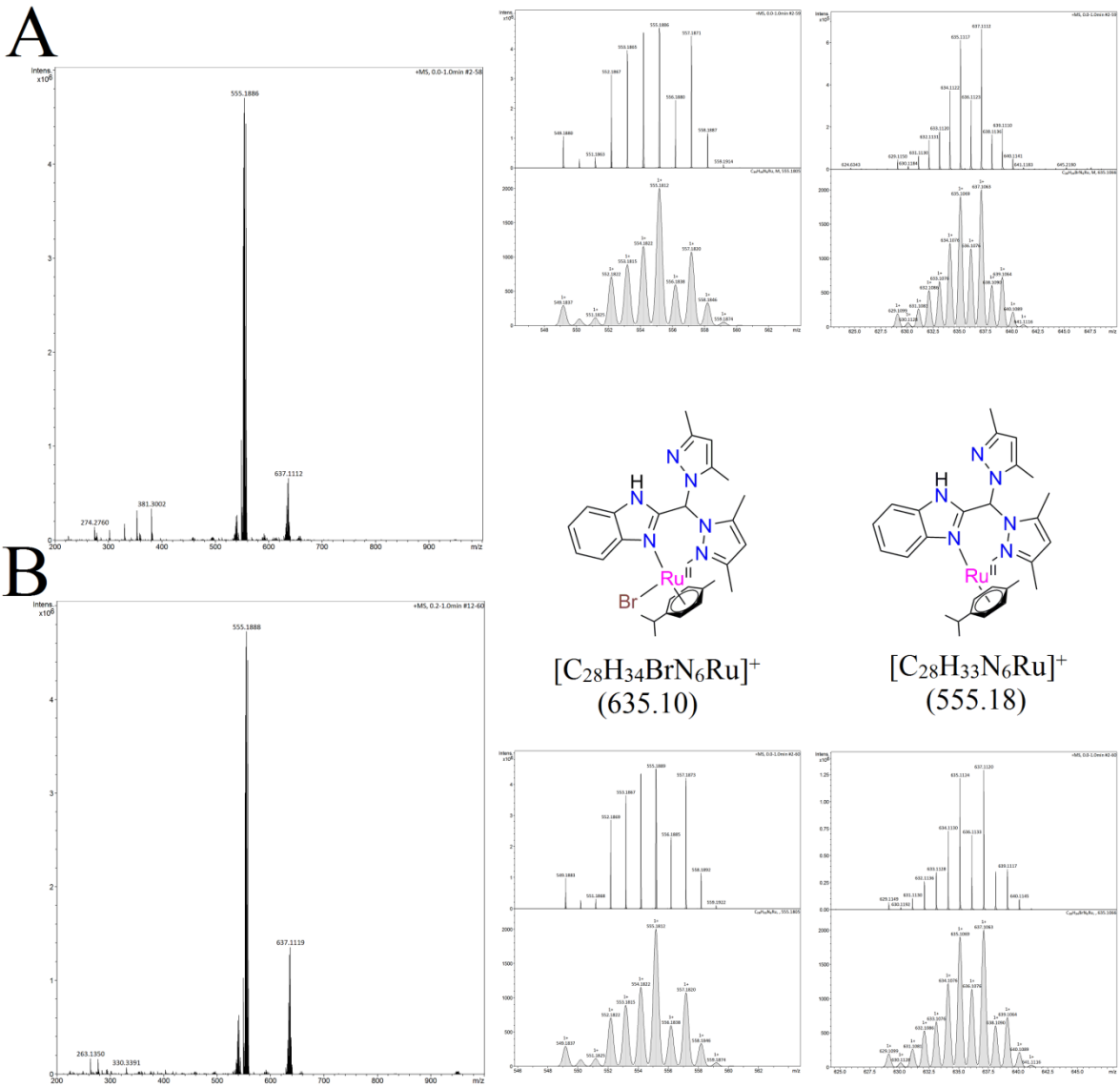

Fig. S20. ESI-MS (+ve mode) spectral traces of **2** in DMSO-d_6 and 10mM phosphate buffer containing 4mM NaCl (pD = 7.4) (2:8 v/v) mixture; A) after 5min and B) 24h of dissolution. Simulated spectra for species of interest are shown in right hand side.

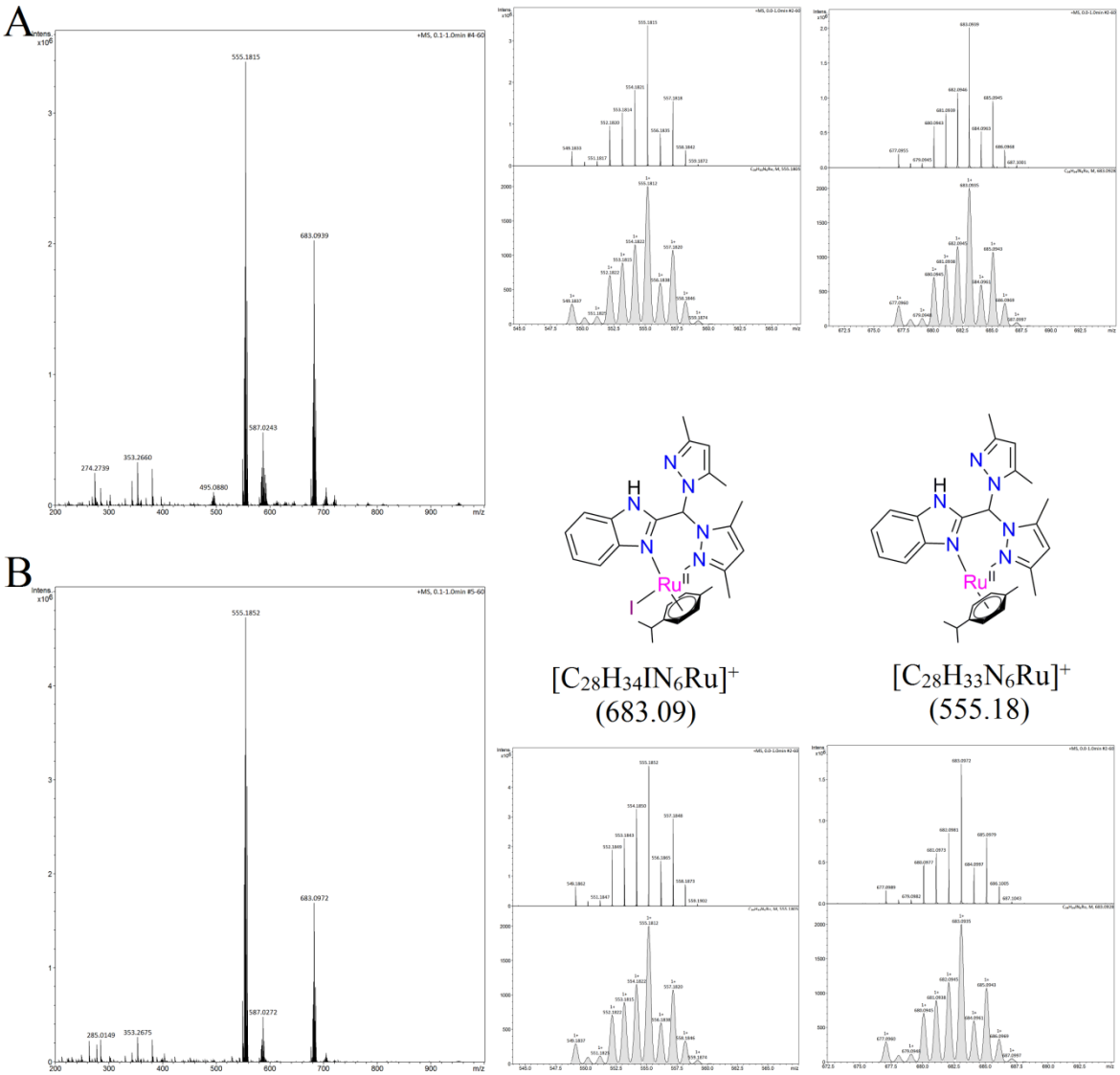

Fig. S21. ESI-MS (+ve mode) spectral traces of **3** in DMSO-d_6 and 10mM phosphate buffer containing 4mM NaCl (pD = 7.4) (2:8 v/v) mixture; A) after 5min and B) 24h of dissolution. Simulated spectra for species of interest are shown in right hand side.

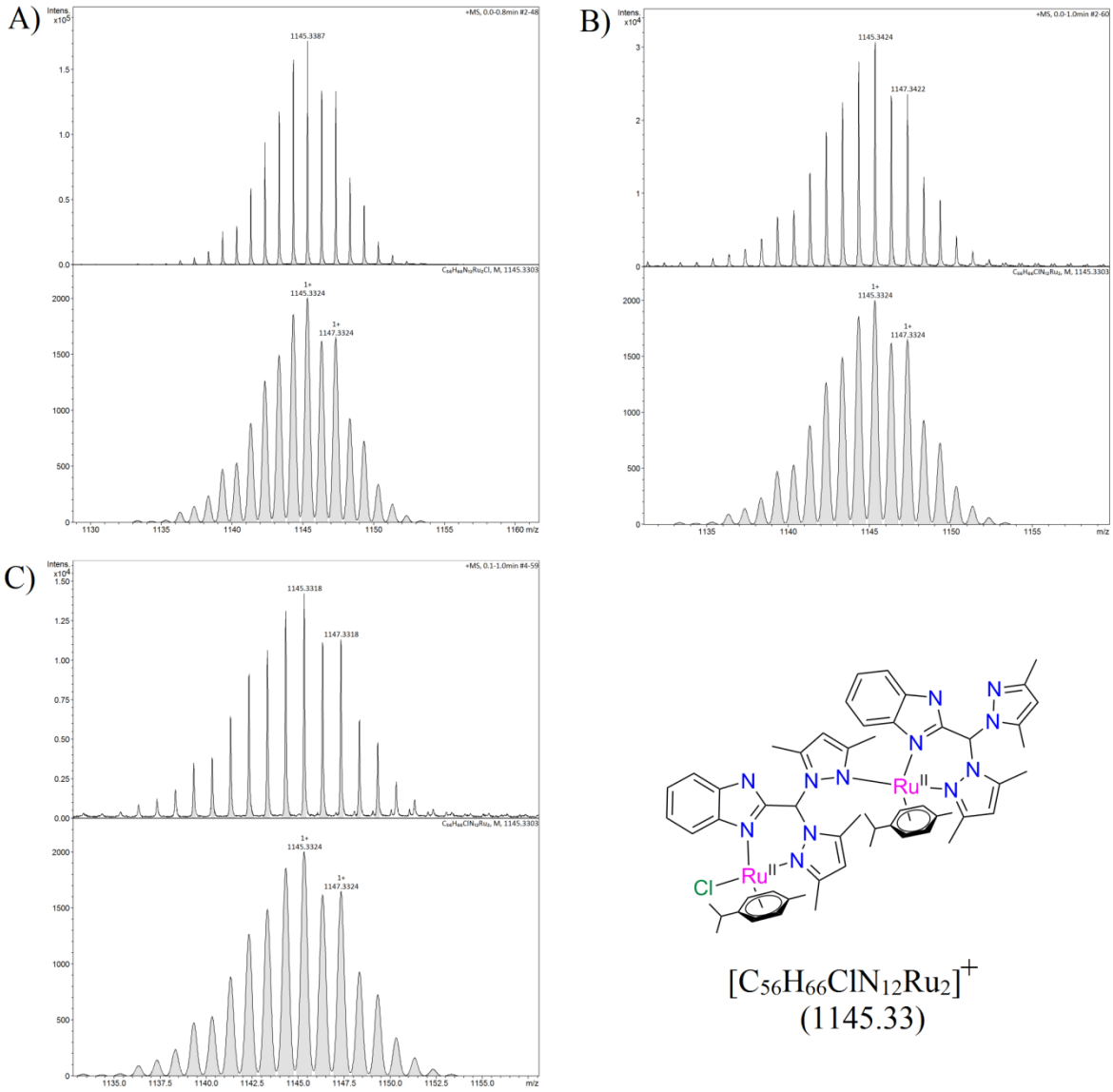

Fig. S22. Spectral simulation of ESI-MS (+ve mode) spectral traces obtained from **1-3** in DMSO-d_6 and 10mM phosphate buffer containing 4mM NaCl (pD = 7.4) (2:8 v/v) mixture after 5min. of dissolution. Only mass corresponding to 1145.33 for dimer (ii) has been shown to prove its existence in solution.

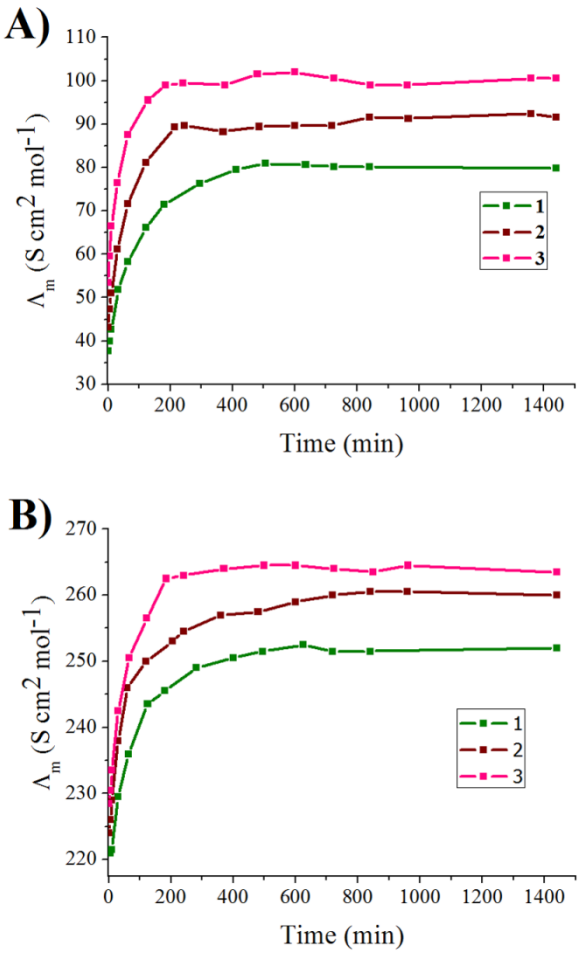

Fig. S23. Change in molar conductance of **1-3** in 1:1 acetonitrile-water mixture. A) in absence, B) in presence of 4mM NaCl.

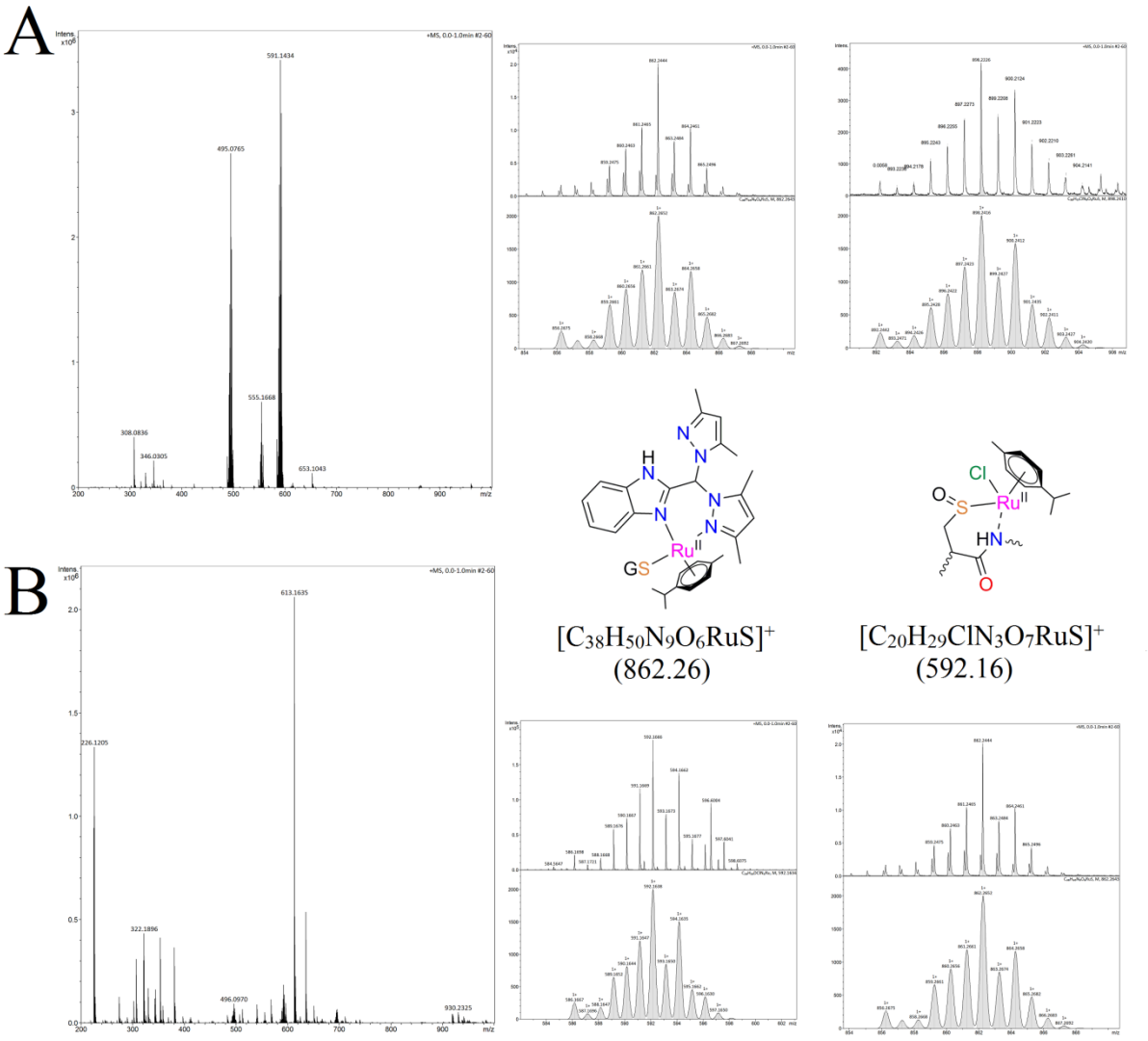

Fig. S24. ESI-MS (+ve mode) spectral traces of **1** and GSH (10eq.) in DMSO-d_6 and 10mM phosphate buffer containing 4mM NaCl (pD = 7.4) (2:8 v/v) mixture; A) after 5min and B) 24h of dissolution. Simulated spectra for species of interest (GSH adduct) are shown in right hand side.

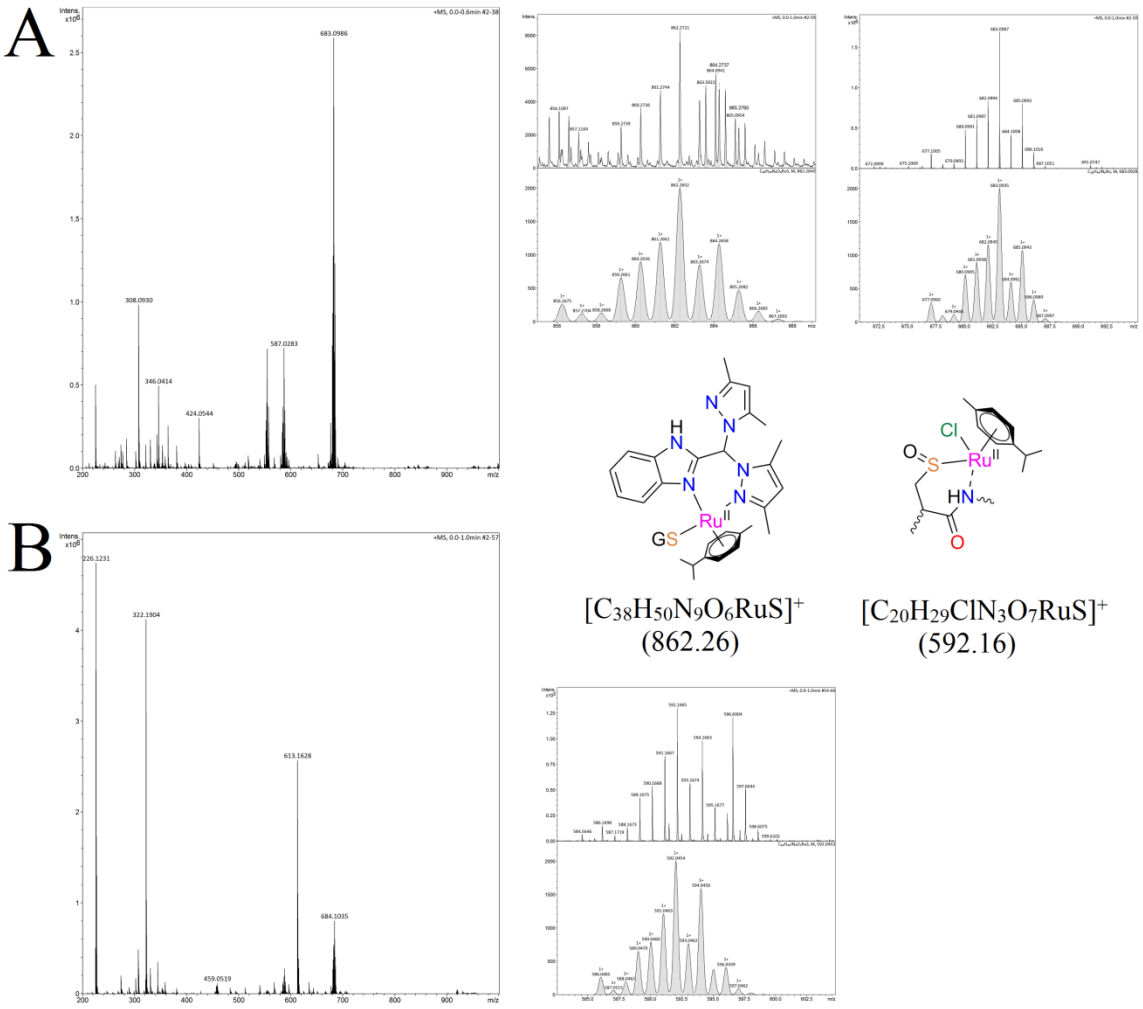

Fig. S25. ESI-MS (+ve mode) spectral traces of **3** and GSH (10eq.) in DMSO-d_6 and 10mM phosphate buffer containing 4mM NaCl (pD = 7.4) (2:8 v/v) mixture; A) after 5min and B) 24h of dissolution. Simulated spectra for species of interest (GSH adduct) are shown in right hand side.

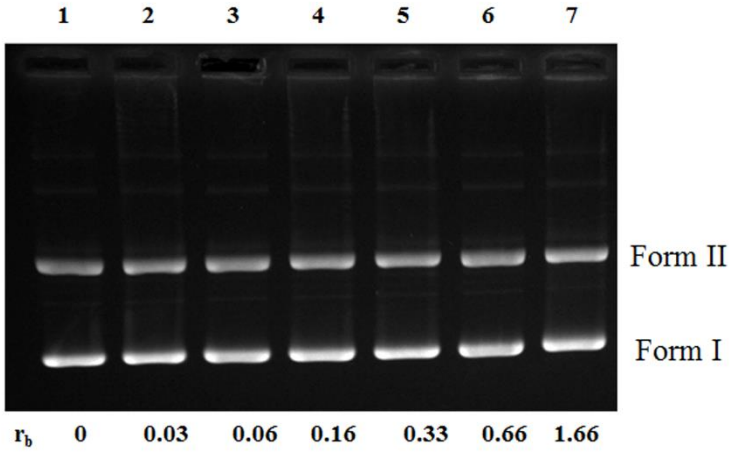

Fig. S26. Agarose gel electrophoresis bands pBR322 plasmid DNA showing unwinding; incubation time = 4h at 37 °C in dark, [DNA] = 30 μM (base pair concentration); DNA was incubated with **1** with r_b = 0 -1.66 (lane 1-7, respectively). DNA loading gel lanes has been shown to confirm loading.

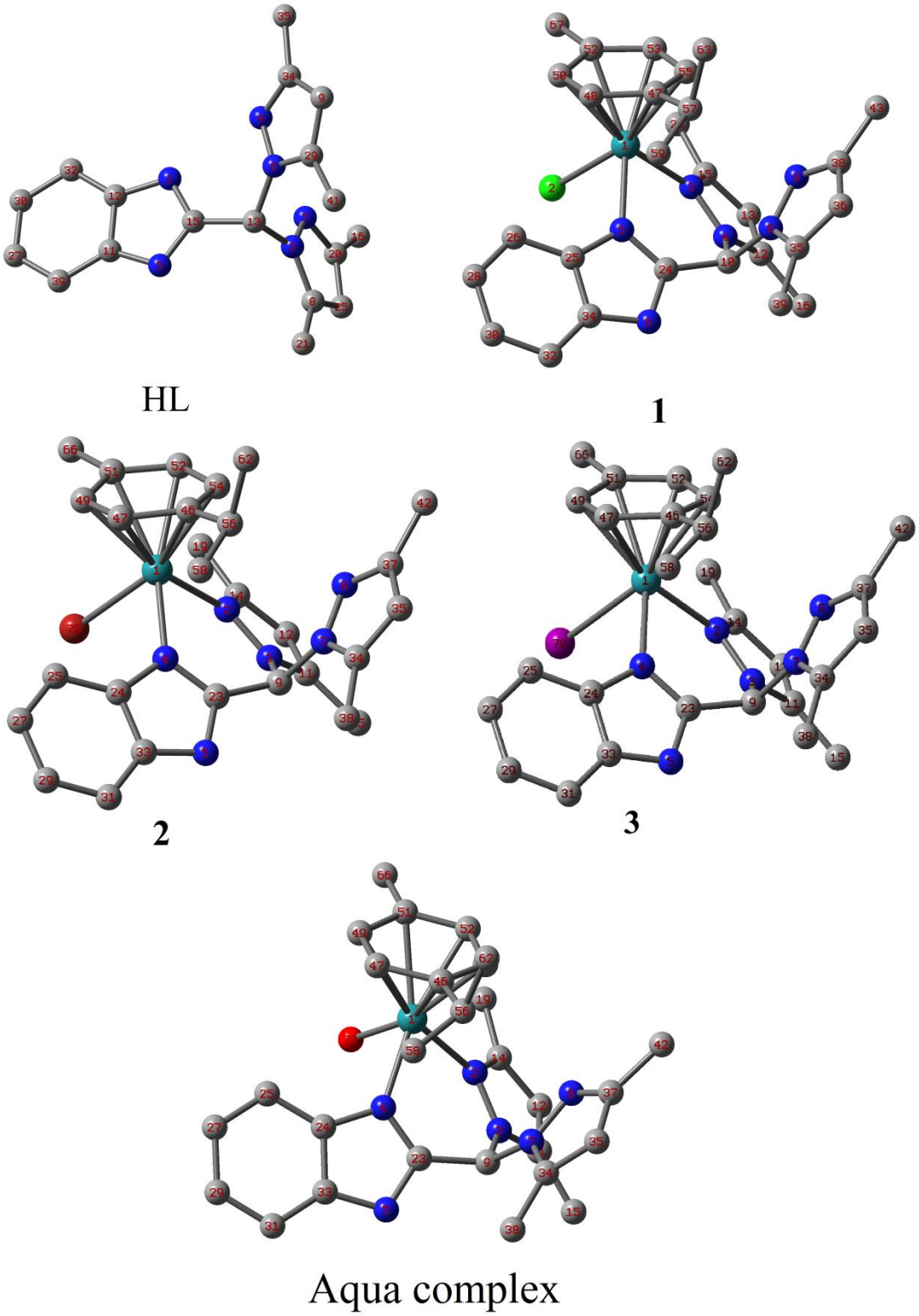

Fig. S27. Representative ball and stick type diagram showing energy optimised structure of HL, **1**-**3** and aqua complex from DFT calculations.

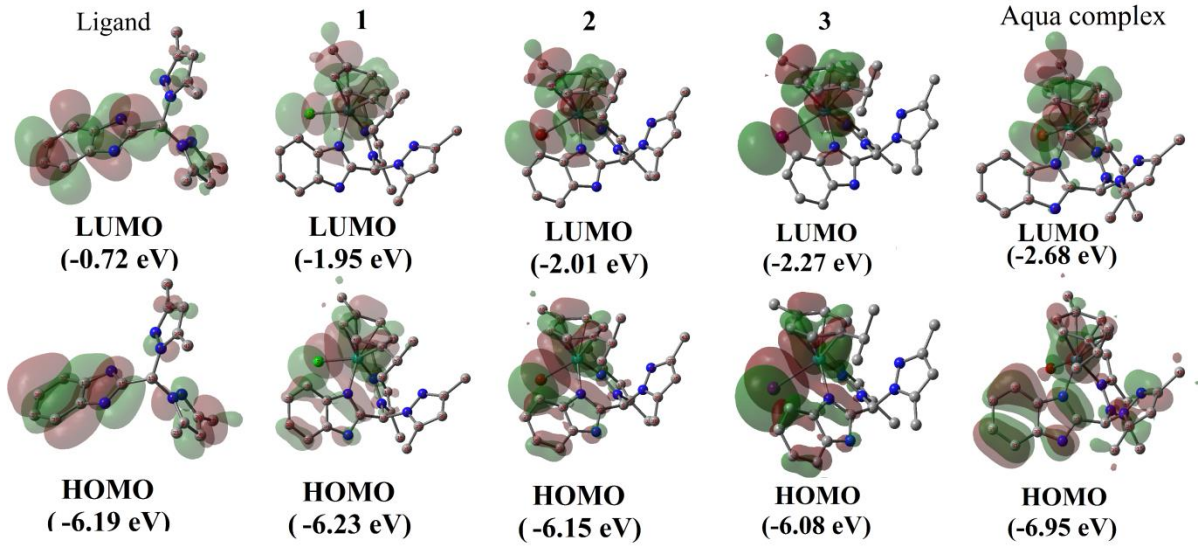

Fig. S28. Frontier molecular orbital diagram with respective energies of HL, **1- 3** and aqua complex obtained from DFT calculation

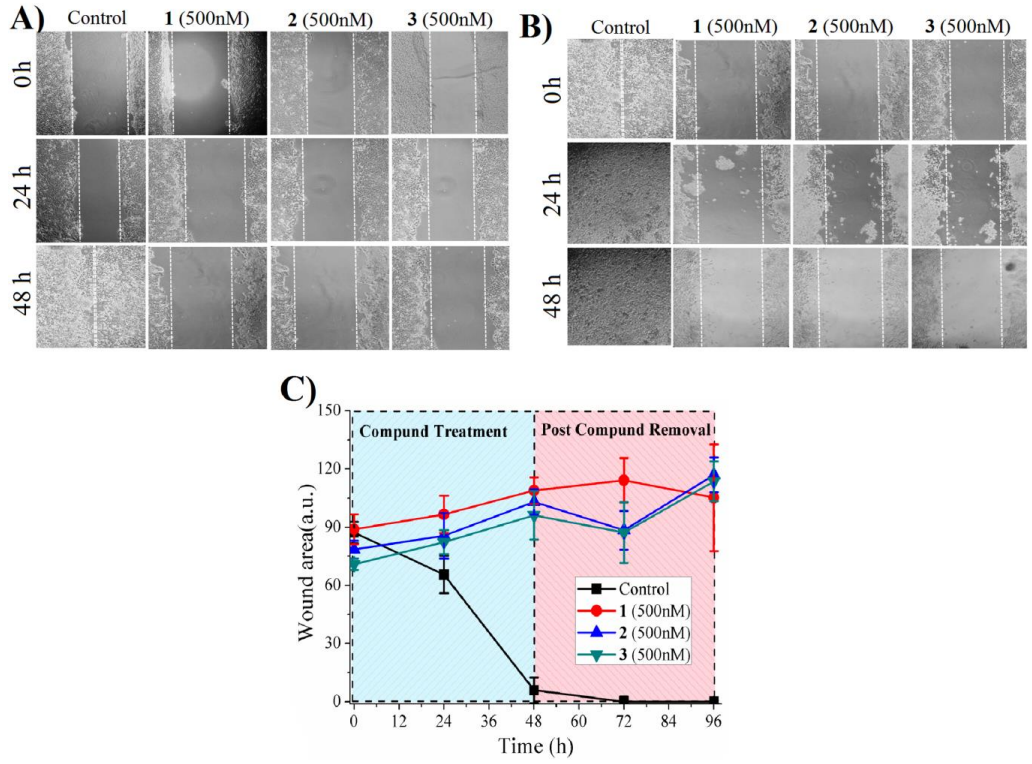

Fig. S29. Wound healing (Scratch) assay showing effect of **1-3** on healing of artificial wound on monolayer of MCF-7 cells, A) upon treatment for 48h; B) up to 48h after removal of complexes with fresh media; C) graphical representation showing trends in wound healing area measured using ImageJ software.

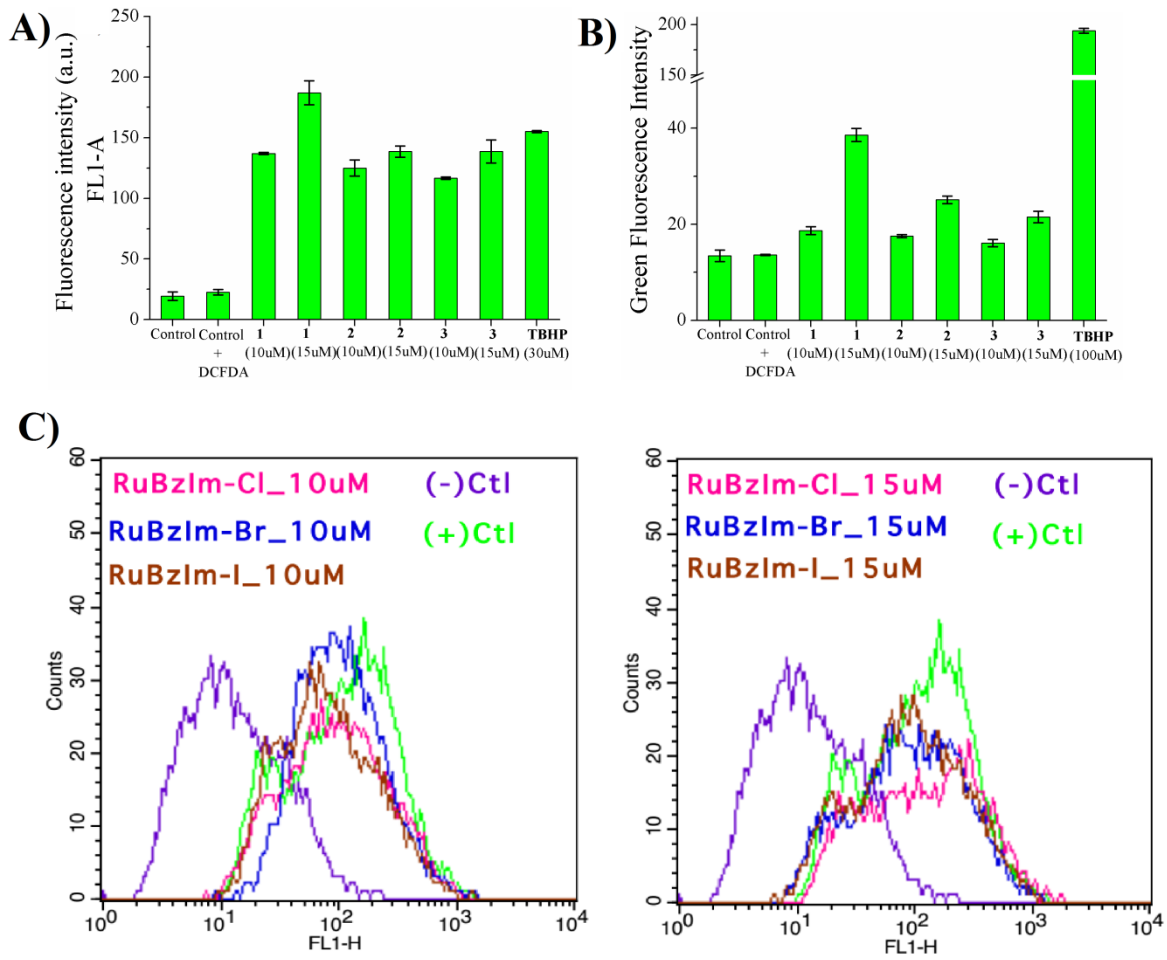

Fig. S30. Typical bar plot green fluorescence intensity of DCFH in presence of ROS *in vitro* (MCF-7) upon treatment with **1-3** at different concentration. A) FL1 channel intensity from FACS data; B) fluorescence measured by micro plate reader coming out from cells, C) histogram plots showing mean intensity of fluorescence (FL1) for different complexes in different concentrations. Tertiary butyl hydrogen peroxide (TBHP) used as positive control in experiment.

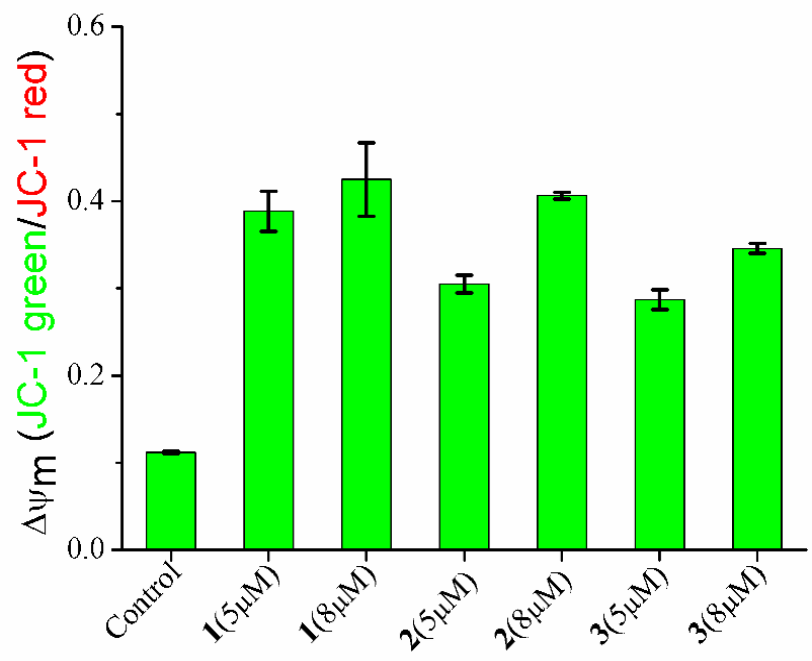

Fig. S31. Typical bar diagram showing FACS data obtained from JC-1 staining for change in mitochondrial transmembrane potential in MCF-7 upon treatment with **1-3** for 24h.

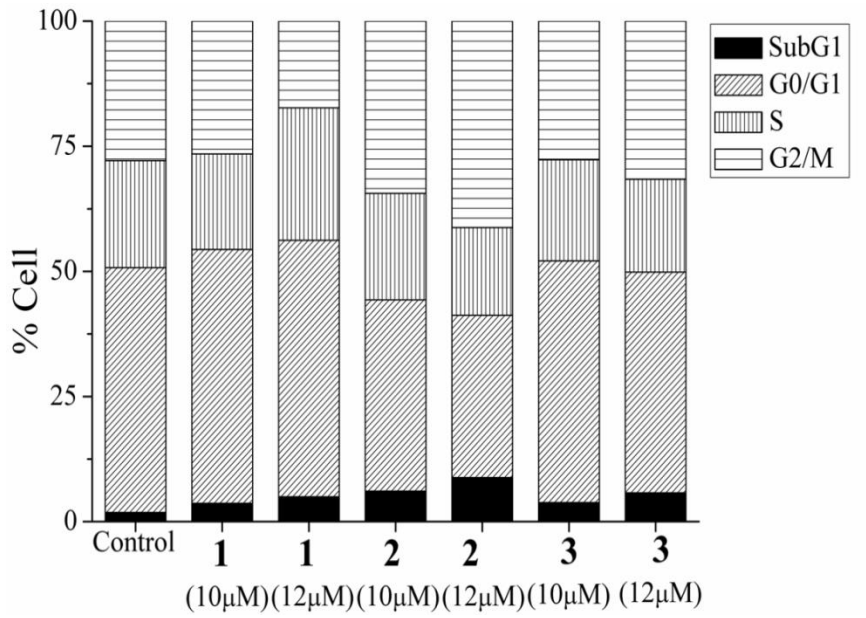

Fig. S32. Typical bar diagram showing population of MCF-7 arrested in different phase in cell cycle upon treatment with **1-3** for 24h.

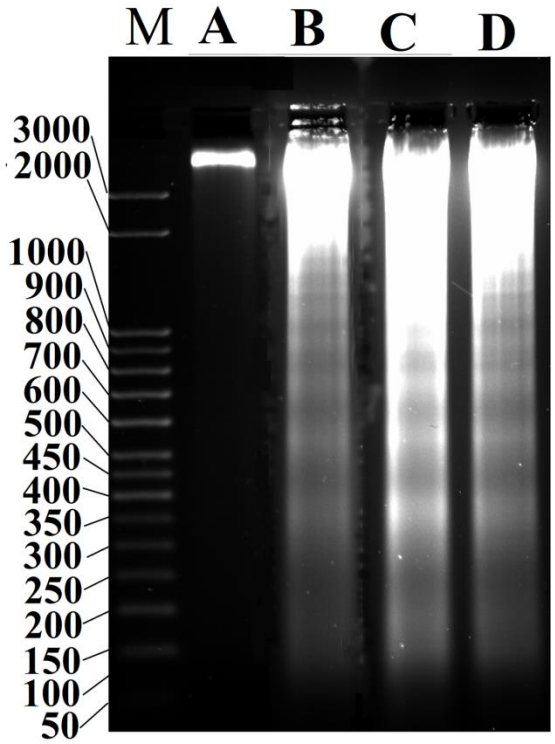

Fig. S33. Agarose gel electrophoresis image of DNA ladder formation after treatment of **1-3** for 24h against MCF-7. A) Control (DMSO ≤0.2%),B) **1**(10μM),C)**2**(10μM), C) **3**(10μM) for 24h. M stands for known base pair (50 bp) marker step ladder for fragment identification.

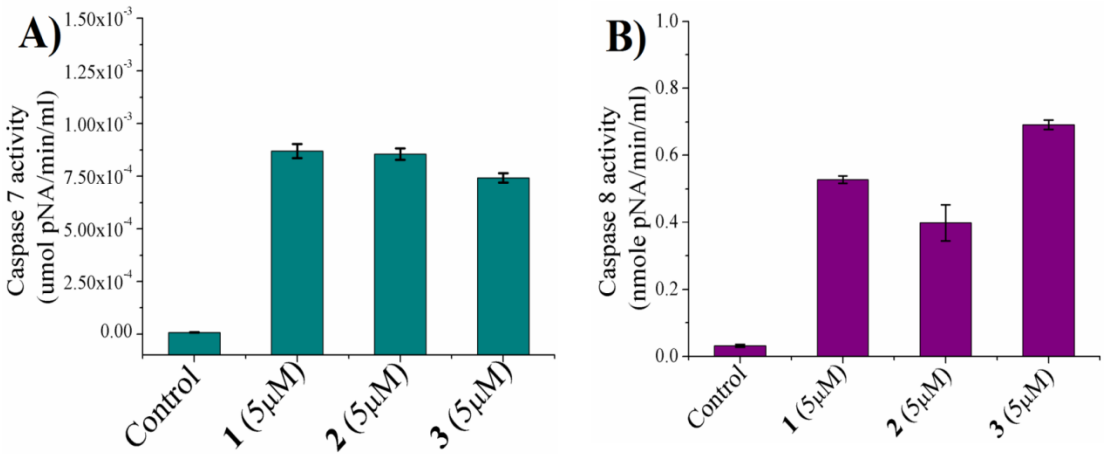

Fig. S34. Colorimetric determination of caspase activation profile in MCF-7 treated with **1-3** for 24h. A) Caspase 7 activation; B) Caspase-8 activation.

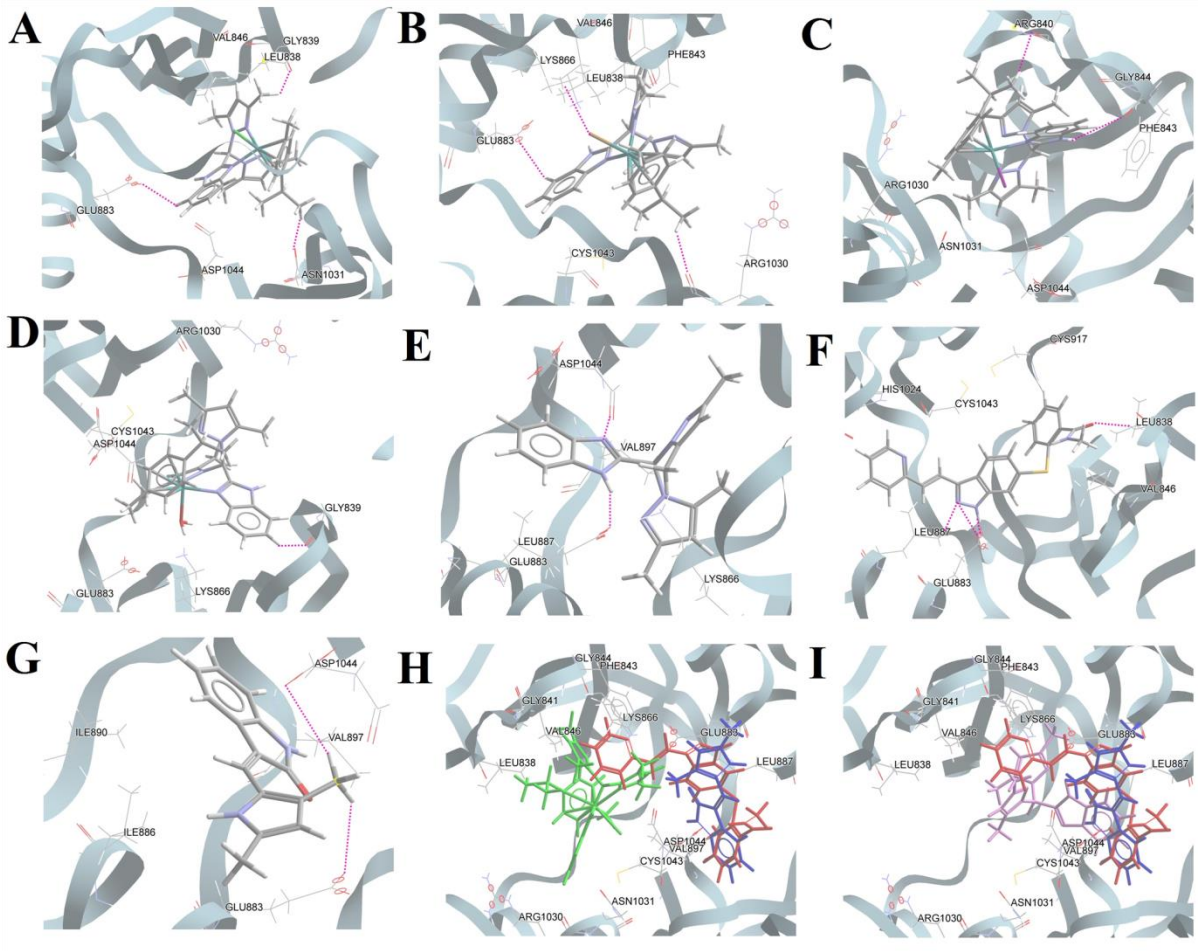

Fig. S35. Representative docking interaction of compounds in kinase binding domain of VEGFR-2 (PDB ID: 1YWN, native structure). A-C) **1-3**, D) aqua complex, E) HL, F)Axitinib, G) SU5416 and cumulative docking structures: H) **1** (green), axitinib (red), SU5416 (blue); i) **1** (green),aqua complex (organge), L (violet), axitinib (red).

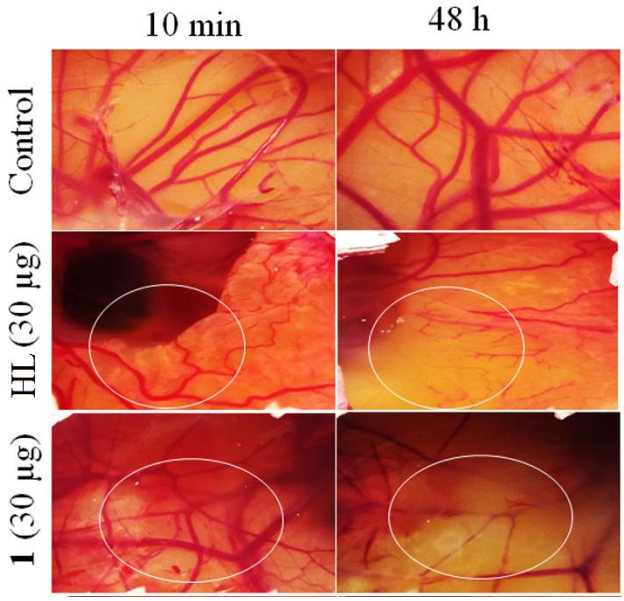

Fig. S36. In ovo anti-vascularisation assay. Inhibition of newer blood vessel formation on treatment with HL, **1** (30 ng) for 48h. White circles points out major affecting area upon treatment.

References

1. Reichmann, M. E.; Rice, C. A.; Thomas, C. A.; Doty, P., A further examination of the molecular weight and size of deoxypentose nucleic acid. *J. Am. Chem. Soc.* **1954,** 76, 3047-53.
2. Marmur, J., A procedure for the isolation of deoxyribonucleic acid from micro.ovrddot.organisms. *J. Mol. Biol.* **1961,** 3, 208-18.
3. Karr. J. P, C. D. S. S. R. G.; Tindall, D. J., Molecular and cellular biology of prostate cancer. . Plenum Press, New York, 199. No. of ISBN: 0 43884 4. *Molecular and cellular biology of prostate cancer. . Plenum Press, New York, 199. No. of ISBN: 0 43884 4* **1989**, 63-64.
4. Lokeshwar, B. L.; Escatel, E.; Zhu, B., Cytotoxic activity and inhibition of tumor cell invasion by derivatives of a chemically modified tetracycline CMT-3 (COL-3). *Curr. Med. Chem.* **2001,** 8, (3), 271-279.
5. Liang, C.-C.; Park, A. Y.; Guan, J.-L., In vitro scratch assay: a convenient and inexpensive method for analysis of cell migration in vitro. *Nat. Protoc.* **2007,** 2, (2), 329-333.
6. Rosman, D. S.; Phukan, S.; Huang, C.-C.; Pasche, B., TGFBR1*6A Enhances the Migration and Invasion of MCF-7 Breast Cancer Cells through RhoA Activation. *Cancer Res.* **2008,** 68, (5), 1319-1328.
7. Nagababu, P.; Barui, A. K.; Thulasiram, B.; Devi, C. S.; Satyanarayana, S.; Patra, C. R.; Sreedhar, B., Antiangiogenic Activity of Mononuclear Copper(II) Polypyridyl Complexes for the Treatment of Cancers. *J. Med. Chem.* **2015,** 58, (13), 5226-5241.
8. An, H.-W.; Qiao, S.-L.; Hou, C.-Y.; Lin, Y.-X.; Li, L.-L.; Xie, H.-Y.; Wang, Y.; Wang, L.; Wang, H., Self-assembled NIR nanovesicles for long-term photoacoustic imaging in vivo. *Chem. Commun. (Cambridge, U. K.)* **2015,** 51, (70), 13488-13491.